Pardo Pascual, JE.; Almonacid Caballer, J.; Ruiz Fernández, LÁ.; Palomar-Vázquez, J.; Rodrigo-Alemany, R. (2014). Evaluation of storm impact on sandy beaches of the Gulf of Valencia using Landsat imagery series. Geomorphology. 214:388-401. doi:10.1016/j.geomorph.2014.02.020.

Evaluation of storm impact on sandy beaches of the Gulf of Valencia using Landsat imagery series

Josep E. Pardo-Pascual,[a*] Jaime Almonacid-Caballer,[a]

Luis A. Ruiz,[a] Jesús Palomar-Vázquez,[a] Raül Rodrigo-Alemany[a]

[a]Geo-Environmental Cartography and Remote Sensing Group
Department of Cartographic Engineering, Geodesy and Photogrammetry
Universitat Politècnica de València.
Camí de Vera s/n, 46022 València, Spain
Corresponding author. Email: jepardo@cgf.upv.es
Phone: 34963877007 (Ext:75537); Fax: 34963877559

Abstract

The impact of storms on sandy beaches and the subsequent recovery process is described from an analysis of the shoreline positions obtained from Landsat 5 TM and Landsat 7 ETM+ imagery. Shoreline extraction is based on an algorithm previously proposed by the authors that enables a positioning accuracy of 5 m root mean square error (RMSE). The impact of six storms registered over a period of seven months (between November 2001 and May 2002) and the beach recovery processes until December 2002 across a 100 km segment of the Gulf of Valencia on the Spanish Mediterranean coast were analysed by comparing 12 shoreline positions.

The multiple shoreline positions obtained from Landsat images provide very useful information for describing the impact of storms and the recovery process across large segments of microtidal coast. This enables the identification of differences not only in the magnitude of change produced by a particular event but also in the cumulative effect associated with several storm events, and in the study of how the beach recovery process takes place. The results show a high level of spatial variability. Beaches with steep slopes experienced fewer changes than shallow slopes. The existence of well developed foredunes in some areas minimised the reduction in the beach width after the storms. Coastal orientation was another important factor in explaining storm impact and the recovery process. This factor affects not only the way the waves interact with the beaches but also the sediment longshore transport: beach regeneration is slower when the transport of sediments is limited by artificial infrastructures (groins, jetties, ports) or natural sediment traps (headlands).

The main limitations of using the proposed methodology to obtain the shoreline position from Landsat images are related to: (i) the precision in the shoreline detection; (ii) the nature of the indicator obtained, that is, the water/land interface; and (iii) the registration instant defined by the image acquisition time. However, the high frequency of the data acquisition and the possibility to cover large coastal areas bring a new perspective that enriches other methods and tools used by coastal scientists.

Keywords: Landsat imagery, Storm impact, Recovery processes, Shoreline evolution, Beach change, GIS tools, Remote Sensing.

1. INTRODUCTION

The impact of storms on beaches induces various morphodynamic responses that significantly modify the coastal landscape over short periods of time (Jiménez et al., 2012). The magnitude of these processes and the resulting changes are controlled by the combination of storm characteristics and coastal geomorphology (Morton, 2002). The type of response is variable depending on the characteristics of the beach even in areas that are similar in appearance. In many areas, the impact of particularly aggressive storms is related to human activities (Leatherman, 1984; Rosati and Ebersole, 1997; Campbell and Jenkins, 2003; Bender and Dean, 2003). There are also cases where high erosion rates on beaches are caused by storms or processes without any human activity (Dolan et al., 1978; Guillén et al., 1999; Schwab et al., 2000; Stive et al., 2002). Since these events often imply major damage in coastal areas, there is a general interest in investigating the factors that determine the impact of storms. As a first step, a proper characterisation of the event is needed, and this means determining the height and energy of the waves (Sénéchal et al., 2009), as well as the maximum water level (Sallenger, 2000). To obtain these parameters from beaches, in addition to wave and sea-level data acquired from nearby shore areas, hindcast modelling methods are used that enable extrapolation of a data time series and its application to areas without available direct measurements (Rangel-Buitrago and Anfuso, 2011; Jiménez et al, 2012; Gervais et al., 2012; Del Río, et al., 2012). However, a definition of the morphological impact of the storm is still needed. This is not usually straightforward, and a variety of approaches can be followed. Some of these approaches are based on beach profile theoretical erosion models, as in the cases of SBEACH (Larson and Kraus, 1989; Wise et al., 1996; Mendoza and Jiménez, 2008), X-BEACH (Roelvink et al., 2009, Plomaritis et al., 2011) or GEOSTORM (Almeida et al., 2011). From these models several parameters are estimated, such as the lost beach profile volume, shoreline recession or maximum flood level during the storm. These models need wave and beach morphology information as input data and, since they are essentially theoretical, the results must be compared to field data measured before and after the storm. In most of the studies, the model output is validated for specific beach segments from where accurate measurements of changes are acquired using systematic profiles (Trifonova et al., 2012; Armaroli et al., 2012), or digital terrain models (DTM) obtained from emerged and submerged areas (Gervais et al., 2012).

Another method for assessing the impact of storms consists of the analysis of the morphological changes in specific coastal segments. This method is based on continuous monitoring of changes before and after

71 the storm and enables the assessment of beach losses and subsequent recovery over time (McLean and
72 Shen, 2006). Several techniques have been used – including the generation of beach profiles (Thom and
73 Hall, 1991; Morton et al., 2002). This technique is effective for the estimation of volume change, but it is
74 limited by the high cost. When applied to large segments, the distribution of profiles tends to be sparse to
75 reduce costs, and this makes it difficult to accurately register variations along the shore (Robertson et al.,
76 2007). A more economic alternative is the registration of changes in the shoreline position (Dolan et al.,
77 1978; Leatherman, 1983; Morton, 1991; Moore, 2000). Traditionally, a shoreline is defined by the high
78 water line or the wet/dry line. However, many different indicators are proposed for this purpose (Boak
79 and Turner, 2005). List et al. (2006) stated that for storm impact studies a datum-based shoreline has
80 advantages over visually interpreted shorelines because its position only shifts in response to sediment
81 transport. Farris and List (2007) concluded that the use of shoreline changes – obtained from datum-based
82 shorelines – is a useful proxy for emerged beach volume change, with the advantage of simplicity, since it
83 can be determined by means of GPS-RTK (Global Positioning Systems-Real Time Kinematic) sensors
84 located on four-wheel vehicles (Pardo-Pascual et al., 2005). These techniques have been used in some
85 studies (Pardo-Pascual et al., 2011; Psuty and Silvera, 2011). However, other authors emphasise that
86 shoreline change is not always representative of the emerged beach volume change. Thus, Robertson et
87 al. (2007) analysed the impact of Hurricane Ivan (September 2004) and the recovery process on a stretch
88 of 25 km near Panama City (Florida), by comparing the beach width changes with respect to the subaerial
89 volume change. The mean shoreline retreat measured after the hurricane was -16.5 m, and the volume
90 change was -30.9 m^3/m. Twenty days later, the shoreline had recovered 10.1 m, while the volume
91 recovered was only 2.7 m^3/m. A new measurement 74 days later showed that the shoreline had recovered
92 only 5.1 m (with respect to the September measure) and the volume recovered was 8.4 m^3/m. Therefore,
93 they concluded that the use of a single date shoreline position is insufficient for characterizing recovery
94 processes.

95 An increasingly popular alternative that enables efficient, fast, and accurate characterisation of the beach
96 shape is the use of airborne LiDAR (light detection and ranging) (Krabill, et al., 2000; Sallenger, et al,
97 2003; Robertson et al., 2007). However, the main constraint is the limited frequency of temporal data that
98 can be provided. In addition, it is usually difficult to take measurements at the peak of a storm and obtain
99 a sufficient number of post-storm measurements to properly monitor the recovery of a beach. Video-
100 monitoring techniques can partially solve these limitations by providing continuous images of the same

area, and while they have been used for storm evaluation (Silva et al., 2009; Sancho-García et al.. 2011) these techniques can only be applied in very local areas, and only two dimensional changes (beach width measurements) can be detected (not three dimensional changes).

All the above- mentioned beach monitoring approaches – those based on field measurements, GPS, LiDAR or video monitoring – provide very useful and accurate information, but they are not practically applicable for monitoring storm response and recovery for large coastal segments due to the high cost involved. In this paper, shoreline automated extraction techniques from a Landsat image series are applied to monitor the impact of storms on beaches and the posterior regeneration. The method employed was proposed by Pardo-Pascual et al. (2012), and involves the sub-pixel extraction of the water/non-water line with an accuracy of approximately 5m RMSE. This method enables the use of Landsat images that have been systematically acquired on a global scale with high frequency since March 1984.

This paper evaluates the ability of this RS methodology to study the impact of storms on beaches, as well as the regeneration process, over long segments of coastline with a variety of beach types by applying a subpixel shoreline extraction method using Landsat imagery. We attempt to discern to what extent using these data for monitoring coastal evolution along wide segments after several coastal storms enables the identification of various morphological responses on the beaches and, thus, the recognition of the main factors that control these geomorphological processes.

2. STUDY AREA AND DATA

Fig. 1. Map of the study area. The green continuous line shows the location of the foredunes near the beach and dotted line (pink line in the web version) shows developed areas near the beach. The numbers indicate the places where submerged profiles were obtained during December 2007.The A, B and C indicate the areas covered by different Landsat images (see table 1). For interpretation of the references to colour in this figure legend, the reader is referred to the web version of this article

The study area is located in the central and southern part of the Gulf of Valencia (Fig. 1) and extends along 100 km of the Spanish Mediterranean coast. This is a sector with small tides: the mean astronomical tide range is 0.18 m, but the maximum water level range registered at the gauge at Valencia in 2009 was 0.73 m (REDMAR, 2009). The dominant waves, obtained from data provided by a non-directional buoy located outside the port of Valencia (39 º 46 'N, 0 º 28'W) and anchored at a depth of 21

m, have low heights and short periods. For the period 1985-2005, the mean significant wave height was 0.78 m and the average peak period was 5.97 seconds (http://www.puertos.es/oceanografia_y_meteorologia/redes_de_medida/index.html). Larger waves develop during storms that are associated with low pressure areas produced by the general westerlies that affect the middle latitudes. The largest storms that affect the Valencian coast have low pressure areas centred on the Gulf of Lyon, but there are also major storms with low pressure areas centred on the Alboran Sea near Gibraltar (Pardo-Pascual 1991). The annual net direction of the longshore current and littoral drift in the Gulf of Valencia is north to south .There is an important sand volume transported to the south every year, estimated in 467,486 m^3 near the port of Valencia (Serra-Peris, 1986). However, because of the orientation of the coast and the angle of the approach of the waves, the transport to the south is more effective when the coast is oriented to the north-east or north and is less effective when the coast is oriented to the north-west. Therefore, longshore transport to the south is more effective north of the Port of Valencia and also along a small segment south of Cape Cullera until the mouth of the river Xuquer. Because of the change of coastal orientation at the southern end of the study area, the littoral drift is practically undefined south of the marina at Goleta d'Oliva (Fig. 1).

From a geomorphological point of view, this sector is dominated by a wide variety of accumulation forms: alluvial fans, flood plains, beach barriers, lagoons, sand dunes and beaches. Most of the beaches are located on beach barriers near marshes. Along the central and southern part of the Gulf of Valencia there are sandy beaches, with small intermittent pebble beaches (Sanjaume, 1985). The formation of the beach barrier has created lagoons, and these are found continuously along the coast. Most of the lagoons located in the study area are actually marshes. Only 'Lake Albufera' just south of Valencia city can still be considered a lagoon, although it has been reduced considerably in size over the last century as a consequence of human action (Sanjaume, 1985).

The shoreline of the area analysed is basically formed by three types of coast: (i) sandy beaches, (ii) the artificially-stabilised coast protected by engineering structures (seawalls, ports, groins); and (iii) small natural cliffs near Cape Cullera. Sandy beaches occupy the largest part of the study zone (80% of the coastline). Approximately 50 km of beaches have buildings and constructions in the backshore – mainly used for holiday purposes – and the other 30 km have coastal dunes along the main alignment of the foredune (Fig. 1). There are also some parts where coastal dunes cover wide areas. The largest is the Devesa del Saler dune field that extends over 850 ha (Sanjaume and Pardo-Pascual, 2011a). There are

161 other significant areas where two or more dune alignments can be found – such as the Oliva municipality
162 and a coastal segment between Xeraco and Gandia.

163 The submerged beach shows significant differences related to the slope profile and the possible existence
164 of submerged bars. A set of submerged profiles made by the Valencia coastal authority (*Dirección*
165 *General de Costas de Valencia*) during December 2007 were analysed and the slope (in degrees) between
166 the shoreline and the -5 m depth isobath was surveyed (Fig. 2). Gentle slopes appear in the accumulative
167 beach sites near the jetties of the ports of Valencia (Patacona, Meliana) or Gandia, and a natural sediment
168 trap as Cape Cullera (North Cullera). Immediately south of these areas, and related with the impact of the
169 littoral drift, are the most eroded beaches – Pinedo, Estany Gran, Brosquil – and these also have steeper
170 slopes.

171

172 *Fig. 2. Profile of the submerged beach slope calculated between elevations 0 and -5 m at different points*
173 *of the studied area in December 2007. The points where the measurements were acquired are indicated.*
174 *North to south locations are ordered from left to right in the figure. The dotted line represents the mean*
175 *slope. Fig. 1 indicates the location of these profiles.*

176

177 3. **IMAGE DATA ANALYSED AND STORM CHARACTERISTICS**

178 The study area was covered by two Landsat standard scenes (199-033 and 198-033) and cloud free
179 Landsat 5 TM and Landsat 7 ETM images downloaded from the USGS archives
180 (http://earthexplorer.usgs.gov/). All images used were catalogued as L1T product (NASA, 2006). This
181 means a level of accuracy better than 0.44 pixels, meaning an error close to 13 m. From the 12 images
182 used (Table 1) only seven cover the complete zone (area C, Fig. 1), another four cover the northern part
183 (66 km) (area B, Fig. 1) and one covers only a small area (30 km) in the central part (area A, Fig. 1).

Images			Storms							
Date	Zone	Tidal level (m)	Duration(h)	H_s(m)	H_{max}(m)	T_p(m)	Tidal level(m)	Max tidal level	Mean meteor. tide(m)	Max meteor. tide(m)
11/8/01	C	-0.02								
11/10/01			49	4.3	8	11.6	0.22	0.35	0.2	0.32
11/14/01			42	3.5	6.6	11.6	0.32	0.48	0.21	0.5
12/14/01			33	3.2	5	11.1	0.03	0.14	0.04	0.1
12/26/01	C	-0.04								
2/19/02	B	-0.18								
3/28/02			39	3.4	7.1	8.1	0.08	0.13	-0.09	0.06
4/2/02			17	2.8	5.6	8	0.06	0.16	0.01	0.06
4/17/02	C	-0.03								

4/24/02	B	-0.15								
5/6/02			41	3	5.6	8.1	0.16	0.27	0.043	0.12
5/19/02	C	-0.16								
5/26/02	B	-0.04								
6/28/02	C	-0.07								
7/29/02	A	0.01								
9/8/02	C	0.14								
10/26/02	C	0.08								
12/29/02	B	-0.08								

Table 1. Acquisition date of the Landsat images, zone (A, B and C in Fig. 1), and tidal elevation at the time of image registration. Information related to storms: duration (in hours), biggest significant height waves (H_s), largest height waves registered (H_m), maximum peak wave period (T_p), mean and maximum sea levels, mean and maximum meteorological tide during the storm.

Data on storm characteristics were obtained from an oceanographic buoy near the Port of Valencia (Fig. 1) and the tide gauge located in the same port. The sea level data were defined considering the mean sea level at the gauge as the zero datum. Here, a storm is understood as defined by Jiménez et al. (2012) for the coast of Catalonia: an event that exceeds a threshold wave height (H_s) of 2 m for a minimum period of six hours. This value was recommended by Mendoza and Jiménez (2008) to define storms in terms of their morphodynamic impact as the minimum condition that induces a significant beach profile response. During the 13 months analysed there were six storms (as defined above): two of them in November 2001, one in December 2001, one in January 2002, one in March 2002, and one in May 2002. The largest storm (Fig. 3) was the first of the series, starting on 10 and 11 November with waves of 4.4 m (H_s); the largest wave was registered at 8 m, and the storm surge was 0.32 m. Another storm started on 14 November, with H_s two days later over 3.5 m and a storm surge of 0.5 m. The next four storms registered lower wave heights and sea level elevations.

Fig. 3. Significant height wave (H_s) and maximum wave height (grey line) during the studied period. The acquisition date (mm/dd/yyyy) of the Landsat images is shown in the dotted line.

The first image (11/08/2001) was taken two days before the 10 November storm and is labelled as a pre-storm situation. The next 11 images were acquired between December 2001 and December 2002 (table 1, Fig. 3, 4).

As explained above, the mean tidal range in the study area is very small, but there are water level changes related to astronomical and meteorological factors. Fig. 4 shows the variation measured at the tide-gauge at the Port of Valencia when Landsat acquired the images, and the moment of maximum water level during the storms.

Fig. 4. Water level change when the Landsat images were acquired, and maximum water level during each analysed storm. The water level has been measured in the tide-gauge located in the port of Valencia, and is referred to the zero level at this gauge.

4. METHODOLOGY

Fig. 5 shows the overall methodological process followed. A time-series of Landsat images (30 m/pixel) were used, together with an accurately orthorectified high-resolution image (0.5 m/pixel) as the geometric reference. This was the input data used for the shoreline extraction algorithm, and it produced a series of georeferenced points every 7.5 m of coast thus defining the detected shorelines per date. The geometric accuracy of the obtained shorelines, understood as the land/water limit and expressed in terms of RMSE, is approximately 5 m depending on the type of image employed: 4.96 m in the case of Landsat TM; 4.69 m for Landsat ETM with high gain radiance; and 5.47 m for Landsat ETM with low gain radiance. The mean error is: -1.66 m , -1.57 m, and -1.22 m, respectively, in each of these image types (values that are close to zero but with a slight landward bias). To convert the points to lines, a customised software program was developed that is described in Section 4.2. The Digital Shoreline Analysis System (Thieler et al., 2009) was then used to determine and analyse the changes in the shoreline.

Fig. 5. Workflow of the methodology used to extract the shorelines

4.1. Shoreline extraction from Landsat imagery

The automated shoreline extraction algorithm is based on a procedure initially described in Ruiz et al. (2007), in which a coarse line is first defined at pixel level using the Landsat middle infrared band 5. A 7x7 neighbourhood around each pixel in this coarse coastline is then analysed to obtain the subpixel line by finding a 2D polynomial that fits the intensity function at that point; and finally, the maximum

238 gradient of this polynomial (representing the land-water interface) is computed. To reduce the effect of
239 variability in the reflectance values of different land covers, a correction coefficient is applied based on
240 the modelling of the local histogram of the image. The final shoreline is obtained as a succession of points
241 every 7.5 m along the coast.
242 Even considering that the accuracy of the original images was better than 13 m, this was not sufficient for
243 our purposes, and the georeferencing of images needed to be improved. This was achieved by applying a
244 single-step discrete Fourier transform (DFT) algorithm, based on the cross-correlation of two images
245 (Guizar-Sicairos et al., 2008) and also referred to as a local up-sampling factor (Wang et al., 2011). The
246 process is fully automated thanks to the specific software developed and no ground control points were
247 required, although a 0.5 m/pixel ortho-image was used as reference. The ortho-image is down-sampled to
248 the Landsat spatial resolution (30 m/pixel) and the Landsat images are geometrically registered to it. The
249 *x* and *y* offsets computed for each Landsat image enable the proper correction of the shoreline points
250 previously extracted from the images. A detailed description of this procedure is given in Pardo-Pascual
251 et al. (2012).
252

253 **4.2. Conversion from points to lines**

254 The shoreline delineation software (SLD) is a Visual Basic-based application that converts the original
255 shoreline points to line geometry. This process involves two main steps: removing anomalous points and
256 line delineation. To remove erroneous points, a coarse reference shoreline (in our case obtained from the
257 National Cartographic database and represented as a dotted line in Fig. 6) was used as the centre line of a
258 buffer (Fig. 6a) that facilitates the elimination of points located too far from the reference line. A
259 shoreline was then delineated as line geometry using the remaining points. For this, different geometric
260 tolerances were applied, such as angle (Fig. 6b) and distance, in order to reduce angularity and smoothen
261 the final line (Fig. 6c). The complete process is automated and a considerable amount of information can
262 be extracted in a reasonable time.

263

264 *Fig. 6. Main steps of the SDL tool for shoreline delineation: a) Anomalous point removal; b) union of*
265 *points that fulfill the criteria of angular tolerance; and c) linear smoothing of the shoreline.*
266

4.3. Measuring and analysing the changes

Once the shorelines were converted to line features, the Digital Shoreline Analysis System (DSAS) application from ArcMap (Thieler et al., 2009) was used to automatically measure the shoreline change at systemic transects that cut the shorelines every 50 m. The changes measured in these transects were then analysed. The rigid coastal segments (seawalls, harbours, groins, etc.) were not analysed as they are man-made and do not respond to natural wave energies and conditions.

4.4. Ancillary data: beach slope measures

Since there was not availability of slope data from the dates of storms, the slope was obtained using aerial LiDAR data acquired in August, 2009. First, the shoreline position was located, then transects perpendicular to the shoreline were obtained every 50 m, and the slope was computed on each of them as the height difference between the shoreline and the point on the transect 5 m landwards.

5. RESULTS

All shorelines were compared in successive transects that measured the changes from the situation prior to the storm (11/08/2001) at eleven subsequent temporal positions in each of the analysed transects. In an initial analysis, the mean changes detected during the period using all the data registered for the eight shorelines that cover the complete area (area C of Fig. 1) were estimated. Fig. 7 shows that on 26 December – just after the largest storms – the average shoreline retreat was about 10 m. The shoreline at 04/19/2002 follows a negative trend. The largest retreat (20 m) was registered in May (05/26/2002), just after the last of the series of five storms after November. Subsequently, as a result of improved wave conditions, the beach width increased, although not reaching the full extension achieved before the series of storms. This behaviour is coherent with the energetic wave conditions experienced during the year, and shows the cumulative effect that successive storms have on most of the beaches – even after taking into account that the first storm was the most energetic.

Fig. 7. Mean shoreline variation of the studied area with respect to the pre-storm situation.

Although this is an interesting result, it is especially important to analyse the spatial variations observed along the 100 km of the studied beach. To achieve this, the study area was divided into 25 sub-areas or zones of different length. In general, they were defined as 5 km in length, except for those areas with features that could change the beach dynamics, such as groin fields, harbour jetties, headlands, etc. In these cases, the segments were subdivided into smaller segments. As a result, the length of the segments ranged from 0.7 to 5 km (Fig. 8). In the electronic version of this paper the reader can open several kmz files to observe in Google Earth the position of the 12 Landsat extracted shorelines and the 25 defined zones (online Supplementary Material).

Fig. 8. Geographical distribution of the 25 different zones – including their local names and lengths.

The mean change between the position of the shore on each date analysed and its location prior to the storm (11/08/01) was calculated for each zone. The change between each date and the pre-storm situation was calculated for each analysed transect, and the mean change of all the transects was then obtained. This value is a good indicator of net coastal change, since very local changes in individual transects are smoothened.

The Hovmoeller plot in Fig. 9 shows the shoreline variations along the coastal segments (Y axis represents the latitude) and the time passed since the first storm analysed (X axis). The position of the 25 zones is scaled and marked. The representation of the last three zones (23-25) is more difficult due to their orientation E-W. The two columns on the right (Fig. 9) represent the mean slope and orientation in each zone. Even if the slope measures correspond to the moment of LiDAR data acquisition – August 2009 - and therefore they are not necessarily representative of the situation in 2001 and 2002 due to the dynamics of the coast, since the mean values of each zone were used the slope characterization can be sufficiently satisfactory. However, there are still some zones where the values are not representative because they have suffered several artificial sand nourishments during the period 2002 to 2009 (e.g. in zones 1 and 6). These zones were not used to evaluate the relationship between slope and shoreline changes.

Fig. 9. Hovmoeller chart of shoreline variations along the coastal segments. This chart shows the loss and gain distribution along latitude and time. In addition, the right columns show the slope and orientation of each zone.

6. DISCUSSION

After describing the shoreline evolution along 100 km of coast, it is important to review the advantages and limitations of the methodology proposed to characterise the impact of storms on beaches, as well as the recovery process. Do the results obtained provide relevant information to assess the effect of storms on beaches and to what extent? To answer these questions, the results must be related to the morphological properties of the beaches, as well as the storm properties, by analysing the main factors that explain the registered morphological changes.

6.1. Main factors that explain differences in morphological changes

The global evolution of the studied area (Fig. 7) shows how the largest retreat of the shoreline is not associated with the highest waves, surges and the longest storms (Table 1) (November 2001), but mainly with the cumulative effect of successive storms. However, as mentioned above, some important differences depend on the geographical area and geomorphic characteristics of the beaches. When we analyze the results (Fig. 9), some remarks about morphodynamic behaviour can be outlined:

i. influence of beach geomorphic conditions,

ii. differing impact on beaches of the November 2001 storm,

iii. differing impact and recovery processes of successive storms, and

iv. influence of water level variations.

Fig. 10. Mean shoreline retreat along the 100 km analysed during the studied period. The dotted line shows the average retreat.

6.1.1. Influence of beach geomorphic conditions

Depending on the geomorphic conditions of the beach, the shore retreat varied greatly. In Fig. 10, the mean beach retreats after the storms of November and December 2001 are represented. This enables the identification of those zones with large variability, such as zones 2, 4, 7, 10, 13, and from 17 to 22. In contrast, zones 1, 3, 8, 9, 15, 16, 23 and 24 showed little variability. The quantification of geomorphological differences in the dynamics of the shoreline enables better interpretation of the factors that affect the behaviour of each sector. Some of these factors have been previously noted by various authors, such as the differing responses observed depending on the types of beaches, especially slope and size of grain sediment (Reyes et al., 1999, Morton, 2002; Haerens et al., 2012). There is an inverse relationship, ($r= -0.71$, $p<0.001$) between the beach mean slope – calculated as explained above - and the mean shoreline change (Fig. 11) which indicates, as expected, that the slope affects the change.

Fig. 11. Relation between the mean slope and the mean beach retreat (in absolute values) obtained per zone for the analysed period. The analysis was made over 78.5% of the length of the beaches, excluding those zones where beach slope changes from 2002 to 2009 were due to artificial sand nourishment.

However, not all areas with small changes are related to the beach slope. Thus, along the beach barrier island of the Albufera lagoon (zones 8 and 9) there are differences in the magnitude of changes in an area with very similar textural characteristics (Sanjaume, 1985). Zones 8 and 9 showed less change (approximately 8.5 m) than zones 10 and 11 (more than 15.5 m). This could be related to the existence of a well-developed foredune in zones 8 and 9, while in zones 10 and 11 the back-beach is formed by buildings and promenades. The dunes of zones 8 and 9 have their bases 2.5 m above mean sea level. Sometimes, during the storms the water level can reach the base of the dune, eroding it and releasing a great volume of sand to the beach (Edelman, 1968; Pye and Blott, 2008). Wave dune erosion returns sand to the littoral system and act to widen the beach and reduce the level of wave action at the dune toe (Davidson-Arnott, 2010). In order to assess this possibility, two parameters were measured: the observed water level (measured at the tide gauge located in the Port of Valencia) and the elevation associated with

the wave run-up (Heathfield et al., 2013). In order to estimate the wave run-up, the elevation which wave swash and set-up attain during storms of high energy on dissipative beaches has been used the following relationship proposed by Ruggiero et al. (2001):

$$R_{2\%} = 0.27\ (SH_sL_0)^{1/2}$$

where $R_{2\%}$ is the beach elevation above the local reference datum that only 2% of extreme water levels will exceed, S, is the beach slope (computed as described above), H_s is the deep water significant wave height (measured at the Valencia buoy) and L_0 is the wavelength (deduced from wave period data measured at the buoy). The beaches of zones 8 and 9 in our study area are also dissipative (Pardo-Pascual and Sanjaume, 1995).

Using this method, it has been estimated that the water elevation at November 12th (first storm) was 2.88 m in zone 8 and 2.87 in zone 9, and two days later (second storm) water reached 2.76 and 2.75 m, respectively. Therefore, as the mean elevation of the dune toe along this area is of 2.5 m the dunes probably were scarped by waves during these storms, supplying sand to the beach during storm events, thus minimising the impact of the storm on the beach width. It is remarkable that, although in zones 8 and 9 the shoreline retreat associated with the November 2001 storm was small, the foredune position suffered a retreat of several metres (Sanjaume and Pardo-Pascual 2011b), as measured by comparing a DEM of the Devesa del Saler dune field that was surveyed in April 2001 with later surveys in 2003 and 2005. Similarly, in zone 12, where 70% of the back-beach is characterized by dunes, the mean shoreline retreat was lower than in the two zones immediately to the north (zones 10 and 11). However, there are other sectors – zones 19 to 22 – where the dunes did not seem to have the same effect or, at least, this has not been evidenced by the mean shoreline retreat registered on the beaches.

6.1.2. Different impact on beaches of the November 2001 storm

The impact of the biggest storms – November 2001 – was very different depending on the zones: i.e., it was greater in zones 1 to 6, 13 and 18, but its impact was slight in the remaining zones (Fig. 9). The two November 2001 storms affected large areas of the Spanish Mediterranean coast. The southern part of the study area was less affected due to the distance from the centre of the storm, which probably led to a lower storm surge than in northern sectors. Some authors had previously remarked that the alongshore

variability of the storm processes, and the geographical location of the storm centre, influence the type and magnitude of storm impacts (Morton, 2002; Haerens et al., 2011). However, in our case, there are two zones (zones 13 and 18) that are distant from the other zones which also suffered substantial shoreline retreat following the storms of November 2001. A factor that could explain this impact is the coastline orientation. Zone 13 – similarly to zones 1 to 6 – is orientated north-south, whereas the other zones are more or less oriented to the NW-SE. Coastal orientation determines longitudinal transport efficiency and seems to have significant influence on the impact of the storm, as Pye and Blott (2008) and Gervais et al. (2012) suggested, particularly in the coastal segment studied here, where the littoral drift is very significant (Sanjaume and Pardo-Pascual, 2005). The differences in coastal orientation are also relevant for understanding why the area closest to the port of Denia (zones 23 to 25) behaved differently to the other areas (Fig. 12).

Fig. 12. Representation of the mean shoreline change in different beach orientations. The impact of the largest storm varies depending on the coastal orientation. The coast orientated north-south includes zones 1 to 6 and 13. Coasts with a northwest-southwest orientation include zones 7 to 22, except the 13th zone, and coasts with a west-east orientation include zones 23 to 25 in the southern part of the area studied.

However, zone 18 (oriented NW-SE) also retreated by more than 25 m on average in comparison with the situation on 8 November. An analysis of the shoreline retreat 8 km north of the Gandia port, from 8 November to 26 December shows that 8 km north of the port (Fig. 13) there is a distinct response in the shoreline position. This difference is probably related to the very different slope of the beach profile due to the cumulative effects of the structure of the port dikes that act as sediment traps (e.g. the case observed in Fig. 13, where the profile 6, measured at the north of Gandia port, presents a slope of 0.75º, while the profile 7 measured 8 km northern from the port presents bigger slope).

Fig. 13. Detail of the changes recorded between 8 November and 26 December 2001 some 8 km north of the port of Gandia. Vertical dotted lines indicate the position of beach profiles made in 2007. In parenthesis is represented the beach slope (see Fig. 2).

6.1.3. Different impacts and recovery processes of successive storms

The succession of storms (Fig. 3 and 4,) – although none was more powerful than the first – generally produced a retreat in the position of the shoreline (Fig. 9) until the weather improved and the storms diminished (June 2002). This occurred in all the study areas except zones 23, 24, and 25, where there is no clear erosive trend during the first part of the year. As explained by Del Río et al. (2012), beaches eroded and flattened by a storm tend to dissipate incident wave energy, which together with the lower wave run-up in gentler slopes could point to a lesser vulnerability to the impact of subsequent storms, and so to a higher threshold for subsequent morphological change. However, flattened beaches allow a given water level to reach areas further inland than in steeper profiles. Our shoreline positions only allow for the registration of two-dimensional change, but not volumetric change. Two response modes to successive storms can be differentiated, as described below:

(a) The coastal sectors basically orientated north-south (zones 1 to 6 and 13), where after the first storms (November and December 2001) the shoreline position remained stable or only changed slightly until June 2002, when a progressive recovery process began. This response mode, where the maximum impact is related to the first storm and successive events do not have much impact, is similar to the recovery model in the Gulf of Cádiz as described by Del Río et al. (2012).

(b) The coastal sector basically oriented northwest-southeast (zones 8 to 23, except zone 13) where successive storms provoke a progressive retreat of the shoreline and achieve a maximum erosion in May 2002. This second response mode shows how several successive medium-energy storms present accumulative impacts on the beach, achieving the maximum erosive impact with the last storm, as discussed by Lee et al., (1998) or Ferreira (2005).

Zone 7 should be classified as a transitional area sharing characteristics of the models (a) and (b). The far southern part of the study area, where the storm impacts were very limited, do not follow any particular response mode.

Our results observed from shoreline changes seem coherent with observations made in the Gulf of Cádiz (Benavente, et al., 2000; Del Río, et al., 2012) where the beach profile morphology was not recovered during calm periods between storms, but began during the summer months when the breeze regime becomes predominant. Moreover, it is interesting to analyse the zones that displayed a clear retreat one year after the first storm. There are eight zones (zones 2, 4, 7, 13, 18, 19, 20 and 21) where the maximum mean recovery exceeded 25 m, and according to the final images less than 70% of this retreat was

recovered. These eight zones have a common characteristic: the longshore transport is very limited (Pardo-Pascual, 1991; Sanjaume and Pardo-Pascual, 2005). Zones 2 and 4 are between groins and ditches and these infrastructures make longitudinal sand nourishment difficult. Zone 7, located immediately south of the port of Valencia, is a clearly starved sector because the jetties of the port act as impervious traps. Zone 13, located south of a headland (Cape Cullera), also acts as a sediment trap except during the largest storms, and receives little sand when the longshore transport comes from the north. Finally, in the four southern zones (18 to 21), the littoral transport from the north is very weak due to the progressive change in the coastal direction in these areas (Pardo-Pascual, 1991; Sanjaume and Pardo-Pascual, 2005). This behaviour is coherent with the main conclusion exposed by Morton et al. (1994) stating that complete recovery depends on the degree of coastal development, which affects the availability of sand to restore the original beach profile. Sometimes, however, if the storm is too heavy, the recovery of the shoreline to the previous positions is not possible, occurring a long term shoreline retreat (Kish and Donoghe, 2013).

6.1.4. Influence of water level variations

In many zones, the biggest change between two registers occurs between the shoreline positions at 05/19/2002 and 05/26/2002 – a mean retreat of about 10 m in the area where data is available. However, there were no storms during these seven days. The shoreline receded between these two dates in all zones, but there were important differences: in zones 17 and 2 the shoreline retreated 25 m and 20 m, respectively. In zones 8, 9, 15 and 16 the retreat was more than 10 m. The rest of the time, where data are available (zones 1 to 18), the retreats were less than 10 m. How can this be explained? An analysis of the water level change (Fig. 4 and Table 1) shows a rise of 12 cm between the two dates. This substantial impact can only be explained if the beach had a very gentle mean slope. After six storms – the last one had a 3.3 m H_s, and a maximum water level of 0.27 m over mean sea level (Table 1 and Fig. 4) and began on 6 May — the beach face may have retained very little gradient. The differences could then be explained by the beach slope differences associated with the impact of the May storm. An interesting contrast is found when analysing the morphological changes after the storms of March and April (with similar wave heights to May storm but slightly lower water level elevation, Table 1 and Fig. 4), and the shoreline changes observed between 17 and 24 April when the mean retreat was only 3 m; despite the fact that tidal elevation fell 12 cm between these two dates. As a result, the beaches slope after the sequence

of storms registered between 28 March and 12 April must be clearly steeper than after the May storm, otherwise the registered shoreline changes cannot be explained.

Therefore, depending on the effective beachface slope, small changes in water level may dramatically affect the shoreline position. This means that considering only the shoreline position can lead us to incorrect deductions about beach evolution, as suggested by Robertson et al. (2007). Furthermore, if this methodology is applied to a coast with greater tidal range, the robustness of the deductions will probably be weaker. Therefore, in order to assess the effect of the tidal range in the impact of coastal storms on the shoreline, this methodology should be appropriately tested using data from other areas.

6.2. Potential and limitations

As mentioned in the introduction section, there are different methods and tools to characterise the impact of storms and beach recovery processes. However, their main limitation is the difficulty of monitoring large coastal areas over a long period of time. A solution is proposed that can frequently monitor a morphological indicator, such as the shoreline position, across large segments of coast. This enables the identification of differences not only in the magnitude of change produced by a particular event, but also in the cumulative effect associated with several storm events, and in the study of how the beach recovery process takes place. This can help specialists in coastal dynamics identify the most relevant factors affecting morphological changes.

The main limitations in using the methodology proposed to obtain the shoreline position from Landsat images are related to: (i) the precision in the shoreline detection; (ii) the nature of the indicator obtained, that is, the water/land interface; and (iii) the registration instant defined by the image acquisition time. Regarding the first issue, although obtaining 5 m RMSE in the shoreline position using 30 m/pixel spatial resolution is an excellent result, this precision is insufficient for every scenario. For example, in areas with low variability (e.g., beaches with high slope, such as those with gravel and pebbles) this precision is insufficient.

Regarding the nature of the indicator, it is obvious that the position of the shore does not always reflect direct sediment changes in the beach profile, and these can be produced as a result of changes in the water level or differences in the beachface slope. Therefore, it would not be safe to make conclusions based on

518 only one shoreline position at a given moment, and it is necessary to study and compare the dynamics and
519 evolution of a temporal series of shorelines.

520 Finally, regarding the third limitation, it is remarkable that this source of information cannot be
521 considered as the best solution when the purpose is to evaluate the maximum real impact of a particular
522 storm. Landsat satellites 5 and 7 have their own data acquisition frequency, and sometimes the first image
523 after a storm is registered so long afterwards that the maximum penetration of the sea waves cannot be
524 determined. Many authors (Masselink et al., 2006; Quartel et al., 2008; Gervais, et al., 2012) indicate that
525 beach changes are difficult to observe when the survey occurs a long time after the event, particularly if
526 the beach recovery is rapid. In this sense, the outcomes presented prove that the impact of a storm, in
527 most of the areas studied, can be clearly detected even 45 days after the event. How long is a 'long time'
528 after the event? The Landsat satellites record a particular scene every 16 days. However, as sometimes
529 happens in some of the studied areas, a part of the territory is recorded in two different scenes. Moreover,
530 between 1999 and 2011, two Landsat satellites were capturing Earth images with different schedules,
531 although from 2003 a malfunction in Landsat 7 meant that the images recorded by the ETM+ sensor
532 showed a systematic linear error. Since February 2013, the Landsat 8 satellite images are also available. It
533 is therefore likely that in many places, especially where clouds are not usual, the repeatability of records
534 provided by the Landsat series may be appropriate for monitoring beach changes caused by the storms.
535 However, sometimes the time between a particular event and the next available image can be too much,
536 or several events may happen between two consecutive available images. These two possibilities can be
537 considered as limitations.

538 Therefore, the changes recorded using shorelines extracted from Landsat imagery can give us key
539 information for understanding the response of sandy beaches to storms, as related to their morphology
540 and geographical position, especially in coastal segments with low tidal ranges. However, there is a risk
541 of producing a confused idea of storm impact or the recovery process if only one shoreline is used. A
542 coherent trend response is obtained when many registers are used, as observed in our study area, and the
543 recovery process can be considered as correctly characterised. Therefore, when comparing several
544 shorelines in short periods of time, a high spatial coherence between positions is observed, and the overall
545 tendency of change is properly characterised. This new source of information is valuable because of the
546 frequency with which information is made available for very large areas.

7. CONCLUSIONS

The possibility of obtaining shoreline positions from Landsat TM/ETM+ images with an accuracy of approximately 5m (RMSE), as proposed by Pardo-Pascual et al. (2012), opens an interesting perspective in the analysis of storm impacts and the beach recovery process. The changes observed along a 100 km coastal segment have been analysed using this method, based on 12 shoreline positions registered during a period of less than 14 months. Up to six storms were recorded during the first months, followed by a long period of calm.

The results show how the beach response in the study area is highly variable, being likely to be conditioned by the morphological differences between the beaches, their geographical location, their main orientations, and any artificial structures in the surrounding area. The detailed analysis of each of the 25 zones studied showed that beaches with major slopes exhibit less change in the shoreline position. Additionally, it has been shown how the existence of dune alignments in some areas mitigates the storm impact and minimises shoreline erosion. It has also been noticed that the influence of the coastal orientation was important in the beach response to a given storm, as shown by the greater impact of the storm on November 2001 on beaches oriented from north to south compared to those oriented NW-SE. Other zones oriented E-W did not undergo significant changes due to this storm. Beach orientation affects how the storm arrives at a beach, but also on the longshore transport efficiency, which is also relevant to the magnitude of the morphological impact. Longshore transport efficiency influences the recovery processes, and these process are slower when the transport of sediments is limited by artificial infrastructures (groins, jetties, ports), natural sediment traps, or simply because of a weak littoral drift caused by the coastal orientation and wave regime. The impact magnitude of the first major storm means that smaller subsequent storms affect the beaches differently. Where changes were substantial after the first storm, the following storms simply maintained the same situation. However, in zones where the effect of the first storm was slight, successive storms produced a progressively larger impact.

A main goal of this work was to evaluate if the use of shorelines automatically extracted from Landsat imagery can provide relevant information about the impact of storms and the recovery process on sandy coasts, especially in areas with low tidal ranges. The results presented show that this source of coastal data gives a new perspective that enriches other methods and tools used by coastal scientists. It is

interesting to note the possibility of re-analysing the effect of storms that took place during the last 30 years in microtidal sandy beaches thanks to the availability of this data source. New tools are available to systematically analyse the response of beaches to storms and their recovery process.

Acknowledgements

The authors appreciate the financial support provided by the Spanish *Ministerio de Ciencia e Innovación* and the Spanish *Plan E* in the framework of the Projects CGL2009-14220-C02-01 and CGL2010-19591. We also thank the *Dirección General de Costas* in Valencia for making available the data for the tests and analysis. Finally, we would like to thank the useful suggestions provided to the anonymous referees and the assigned editor, which enabled us to improve the quality of this paper.

REFERENCES

Almeida, L.P., Ferreira, Ó., Taborda, R., 2011. Geoprocessing tool to model beach erosion due to storms: application to Faro beach (Portugal). Journal of Coastal Research, SI 64, 1830-1834.

Armaroli, C., Ciavola, P., Perirni, L., Calabrese, L., Lorito, S., Valentini, A., Masina, M., 2012. Critical storm thresholds for significant morphological changes and damage along the Emilia-Romagna coastline, Italy. Geomorphology, 143-144, 34-51.

Benavente, J. , Gracia, F.J., López-Aguayo, F., 2000. Empirical model fo morphodynamic beachface behaviour for low-energy mesotidal environments. Marine Geology, 167, 375-390.

Bender, C.J., Dean, R.D., 2003. Wave field modification by bathymetric anomalies and resulting shoreline changes: a review with recent results. Coastal Engineering, 49, 125-153.

Boak, E.H. & Tunner, I.L., 2005. Shoreline definition and detection: a review. Journal of Coastal Research, 21 (4), 688-703.

Campbell, T.J., Jenkins, M.F., 2003. Design considerations for hot spot erosion areas on beach nourishment projects. 28th International Conference on Coastal Engineering. World Scientific, London, 3642-3648.

Davidson-Arnott, R., 2010. Introduction to coastal processes and geomorphology. Cambridge University Press, Cambridge.

Del Rio, L., Plomaritis, T.A., Benavente, J., Valladares , M., Ribera, P., 2012. Establishing storm thresholds fot the Spanish Gulf of Cádiz coast. Geomorphology¸ 143-144, 13-23.

Dolan, R. Hayden, B.P., Heywood, J., 1978. A new photogrammetric method for determining shoreline erosion. Coastal Engineering, 2, 21-39.

Dolan, R. Hayden, B.P., Rea, C., Heywood, J., 1979. Shoreline erosion rates along the middle Atlantic coast of the United States. Geology¸ 7, 602-606.

Edelman, T.1968. Dune erosion during storm conditions. Proeceedings of the 11th Conference on Coastal Engineering, London, vol. 2, 719-722.

611 Farris, A.S., List, J.L., 2007. Shoreline change as a proxy for subaerial beach volume change. Journal of
612 Coastal Research, 23 (3), 740-748.

613 Ferreira, O., 2005. Storm groups versus extrem single storms: predicted erosion and management
614 consequences. Journal of Coastal Research, SI 42, 421-227.

615 Gervais, M., Balouin, Y,, Belon, R., 2012. Morphological response and coastal dynamics associated with
616 major storm events along the Gulf of Lions Coastline, France. Geomorphology, 143-144, 69-80.

617 Guillen, J., Stive, M.J.F., Capobianco, M., 1999. Shoreline evolution of the Holland coastal on a decadal
618 scale. Earth Surface Processes and Landforms, 24, 517-536.

619 Guizar-Sicairos, M., Thurman, S. T., & Fienup, J. R., 2008. Efficient subpixel image registration algorithms.
620 Optics Letters, 33(2), 156–158.

621 Haerens, P.,Bolle, A., Trouw, K., Houthuys, R., 2012. Definition of storm thresholds for significant
622 morphological change of the sandy beaches along the Belgian coastline. Geomorphology, 143-144,
623 104-117.

624 Heathfield, D.K., Walker, I.J., Atkinson, D.E., 2013. Erosive water level regime and climatic variability
625 forcing of beach-dune systems on south-western Vancouver Island, British Columbia, Canada. Earth
626 Surface Processes and Landforms, 38, 751-762.

627 Jiménez , J.A., Sancho-García, A., Bosom, E., Valdemoro, H.I., Guillén, J., 2012. Storm-induced damages
628 along the Catalan coast (NW Mediterranean) during the period 1958-2008. Geomophology, 143-144,
629 24–33.

630 Kish, S.A., Donoghue, J.F. 2013. Coastal response to storms and sea-level rise: Santa Rosa Island, Northwest
631 Florida, U.S.A., Journal of Coastal Research, SI 63. 131-140.

632 Krabill, W., Wright, C., Swift, R., Frederick, E., Manizade, S., Yungel, J., Martin, C., Sonntag, J., Duffy, M.,
633 Hulslander, W.,, Brock, J., 2000. Airborne laser mapping of Assateague National Seashore Beach.
634 Photogrammetric Engineering & Remote Sensing, 66, 65-71.

635 Larson, M., Kraus, N.C., 1989. SBEACH: Numerical model for simulating storm-induced beach change.
636 CERC-89-9, US Corps of Engineers, Vicksburg.

637 Leatherman, S.P., 1983. Shoreline mapping: a comparison of techniques. Shore and Beach, 51, 28-33.

638 Leatherman, S.P., 1984. Shoreline evolution of North Assateague Island, Maryland. Shore and Beach, 52, 3-
639 10.

640 Lee, G. Nichols, R.J., Birkemeier, W.A,, Leatherman, S.P., 1995. A conceptual fairweather-storm model of
641 beach nearshore profile evolution at Duck, North Carolina, USA. Journal of Coastal Research, 11 (4),
642 1157-1166.

643 Lee, G. Nicholls, R.J., Birkemeier, W.A., 1998. Storm.driven variability of the beach-nearshore profile at
644 Duck, North Carolina, USA, 1981-1991. Marine Geology, 148, 163-177.

645 List, J. H., Farris, A.S., Sullivan, Ch., 2006. Reversing storm hotspots on sandy beaches: spatial and temporal
646 characteristics. Marine Geology, 226, 261-279.

647 Masselink, G., Kroon, A., Davidson-Arnott, R.G.D., 2006. Morphodynamics of intertidal bars in wave-
648 dominated coastal settings—a review. Geomorphology 73, 33–49.

649 McLean, R., Shen, J.S., 2006. From foreshore to foredune: Foredune development over the last 30 years at
650 Moruya Beach, New South Wales, Australia, Journal of Coastal Research, 23, 1: 28-36.

651 Mendoza E.T., Jiménez J.A., 2008. Coastal storm classification on the Catalan littoral (NW Mediterranean).
652 Ingeniería Hidráulica en México, 23(2), 23–34

653 Moore, L.J., 2000. Shoreline mapping techniques. Journal of Coastal Research, 16(1), 111-124.

Morton, R.A., 1991. Accurate shoreline mapping; past, present and future. Coastal Sediments. American Society of Civil Engineers, 1, 997-1010.

Morton, R.A., Paine, J.G, Gibeaut, J.G. 1994. Stages and durations of post-storms beach recovery, southeastern Texas coast, U.S.A., Journal of Coastal Research, 10,884-908.

Morton, R.A., 2002. Factors controlling storm impacts on barrier and beaches: a preliminary basis for real-time forecasting. Journal of Coastal Research, 19, 560-573.

NASA (2006). Landsat 7 science data users handbook, (on-line). available on. http:// landsathandbook.gsfc.nasa.gov/pdfs/Landsat7_Handbook.pdf (September, 2011)

Pardo-Pascual, J.E., 1991. La erosión antrópica en el litoral valenciano. Conselleria d'Obres Públiques, Urbanisme i Transports, Generalitat Valenciana, Valencia.

Pardo-Pascual, J.E., Sanjaume, E. 1995. Caracterización de las playas valencianas a partir del parámetro escalar de surf. III Jornadas Españolas de Ingeniería de Costas y Puertos, Universitat Politècnica de València, 614-628.

Pardo-Pascual, J.E., García-Asenjo, L., Palomar Vázquez, J., Garrigues-Talens, P., 2005. New methods and tools to analyze beach-dune system evolution using a Real-Time Kinematic Global Positioning System and Geographic Information Systems. Journal of Coastal Research, SI: 49, 34-39.

Pardo-Pascual, J.E.; Palomar-Vázquez, J.M., García-Asenjo Villamayor, L., Garrigues Talens, P., 2011. Determinación de la tendencia evolutiva en un segmento de playa basándose en múltiples levantamientos tridimensionales. Avances en Geomorfología Litoral, VI Jornadas de Geomorfología Litoral, Tarragona, 493-496.

Pardo-Pascual, J.E., Almonacid-Caballer, J., Ruiz, L.A., Palomar-Vázquez, J., 2012. Automatic extraction of shorelines from Landsat TM and ETM multi-temporal images with subpixel precision. Remote Sensing of Environment, 123, 1-11.

Plomaritis, T.A., Del Rio, L, Benavente, J., 2011. Validating and estimating storm threshold using a single Environmental Parameter: The case of Cadiz coast. Journal of Coastal Research, SI 64, 1876-1880.

Psuty, N.P. , Silvera, T.M., 2011. Tracking coastal geomorphological change: an application of protocols to collect geotemporal data sets at the national level in the US. Journal of Coastal Research, SI 64, 1253-1257.

Pye, K. , Blott, S.J., 2008. Decadal-scale variation in dune erosion and accretion rates: an investigation of the significance of changing storm tide frequency and magnitude on the Sefton coast, UK. Geomorphology. 102, 652-666.

Quartel, A. , Kroon, A., Ruessink, B.G. 2008. Seasonal accretion and erosion patterns of a microtidal sandy beach, Marine Geology, 250, 19-33.

Rangel-Buitrago, N, Anfuso, G., 2011. Coastal storm characterization and morphological impacts on sandy coasts. Earth Surf. Process. Landforms, 36, 1997–2010.

REDMAR (2009): Red de mareógrafos de Puertos del Estado (Informe anual 2009), Dirección de Relaciones Institucionales e Innovación Tecnológica, Puertos del Estado, 395 pp. (available in: http://calipso.puertos.es//BD/informes/anuales/redmar/REDMAR2009.pdf, last access in February 2013).

Reyes, J.L., Martins, J.T, Benavente, J. ,Ferreira, Ó., Gracia, F.J., Alveirinho-Dias, J.M., López-Aguayo, G. 1999. Gulf of Cádiz beaches: a compartive response to storm events. Boletín Instituto Español de Oceanografía, 15, 221-228.

Robertson, W. V., Zhang, K., Whitman, D., 2007. Hurricane-induced beach change derived from airborne laser measurements near Panama City, Florida. Marine Geology, 237, 191-205.

Roelvink, D., Reniers, A., van Dongeren, A., de Vries, J. V., McCall, R., Lescinski, J., 2009. Modelling storm impacts on beaches, dunes and barrier islands. Coastal Engineering, 56(11-12), 1133–1152.

Rosati, J.D., Ebersole, B.A., 1997. Littoral impact of Ocean City Inlet, Maryland, USA. Proceed.25th International Conference on Coastal Engineering. American Society Civil Engineering, New York, 2779-2792.

Ruggiero, P., Komar, P.D., McDougal, W.G., Marra, J.J., Beach, V.A. 2001. Wave runup, extreme water level s and the erosion of properties backing beaches. Journal of Coastal Research, 17 (2), 407-419.

Ruiz, L. A., Pardo-Pascual, J. E., Almonacid-Caballer, J., Rodríguez, B., 2007. Coastline automated detection and multi-resolution evaluation using satellite images. Proceedings of coastal zone 2007, Portland (Oregon)

Sallenger, A.H., 2000. Storm impact scale for barrier islands. Journal of Coastal Research, 16, 890-895.

Sallenger, A.H., Krabill, W., Swift, R., Brock, J., List, J., Hansen, M., Holman, R.A., Manizade, S., Sontag, J., Meredith, A., Morgan, K., Yunkel, J.K., Frederick, E., Stockdon, H., 2003. Evaluation of airborne scanning lidar for coastal change applications. Journal of Coastal Research, 19, 125-133.

Sancho-García, A.. Ruessink, B.G, Guillén, J. 2011. Storm-surge inundation along a multibarred beach, *Journal of Coastal Research,* SI 64, 1911-1915..

Sanjaume, E., 1985: Las costas valencianas. Sedimentología y morfología. Universitat de València, Valencia.

Sanjaume, E., Pardo-Pascual, J.E, 2005 Erosion by human impact on the Valencian coastline. Journal of Coastal Research, SI, 49, 76-82.

Sanjaume, E., Pardo-Pascual, J.E., 2011a. Las dunas de las costas valencianas. In: Sanjaume, E. and Gracia Prieto, F.J. (Eds.), Las dunas en España¸ Sociedad Española de Geomorfología, 227-262.

Sanjaume, E., Pardo-Pascual, J.E., 2011b. Las dunas de la Devesa del Saler. In: Sanjaume, E. and Gracia Prieto, F.J. (Eds.), Las dunas en España¸ Sociedad Española de Geomorfología, 263-284.

Schwab, W.C., Thieler, E.R., Allen, J.R., Foster, D.S., Swift, B.A., Denny, J.F., 2000. Influence of inner-continental shelf geologic framework on the evolution and behaviour of the barrier-island system between Fire Island Inlet and Shinnecock Inlet, Long Island, New York. Journal of Coastal Research, 16, 408-422.

Sénéchal, N., Gouriou, B., Castelle, B., Parisot, J.-P., Capo, S., Bujan, S., Howa, H., 2009. Morphodynamic response of a meso- to macro-tidal intermediate beach based on a long term data set. Geomorphology, 107 (3-4), 263-274.

Serra-Peris, J. 1986. Procesos litorales en la costa de Castellón. Ph D. Unpublished. ETS Ingenieros de Caminos, Canales y Puertos, Universitat Politècnica de València, Valencia.

Silva, A. , Taborda, R., Castelao, J., Freire, P. , 2009. DTM extraction using video-monitoring techniques application to the fetch limited beach, Journal of Coastal Research, SI 56: 203-207.

Stive, M.J.F., Aarninkhof, S.G.-J., Hamm, L., Hanson, H., Larson, M., Wijnberg, K.M., Nicholls, R.J., Capobianco, M., 2002. Variability of shore and shoreline evolution. Coastal Engineering, 7: 211-235.

Thieler, E. R., & Danforth, W. W., 1994. Historical shoreline mapping (I): Improving techniques and reducing positioning errors. Journal of Coastal Research, 10(3), 549–563.

Thieler, E.R., E.A. Himmelstoss, J.L. Zichichi, Ayhan, E., 2009. Digital Shoreline Analysis System (DSAS) version 4.0 An ArcGIS extension for calculating shoreline changes. U.S. Geological Survey Open-File Report, 2008-1278.

Thom, B.G., Hall, W., 1991. Behaviour of beach profiles during accretion and erosion dominated periods. Earth Surface Processes and Landforms, 16: 113-127.

Trifanova, E.V., Valchev, N.N.,. Andreeva, N.Y.,, Eftimova, P.T., 2012. Critical storm thresholds for morphological changes in the western Black Sea coastal zone. Geomorphology 143-144, 81-94.

743 Wang, C. , Zhao, C. , Yang, J., 2011. Local Upsampling Fourier Transform for High Accuracy Image
744 Rotation Estimation. Advanced Materials Research, 268-270, 1488-

745 Wise, R. S., Smith, S.J, Larson, M., 1996: SBEACH. Numerical model for simulating storm-induced beach
746 change. CERC, US Army Corps of Engineers, Vicksburg.

Figure 1 (colour)

Click here to download high resolution image

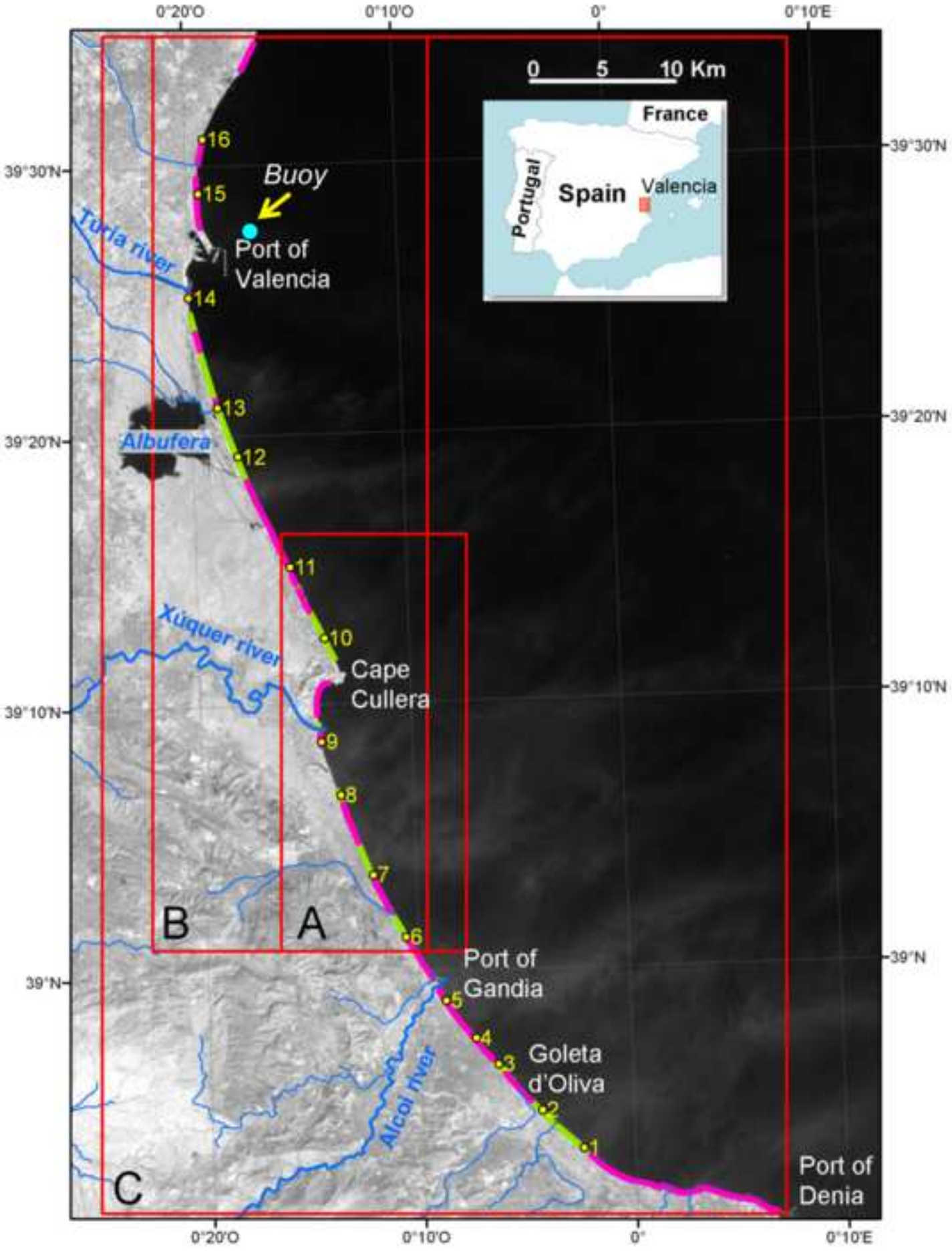

Figure 2 (colour)
Click here to download high resolution image

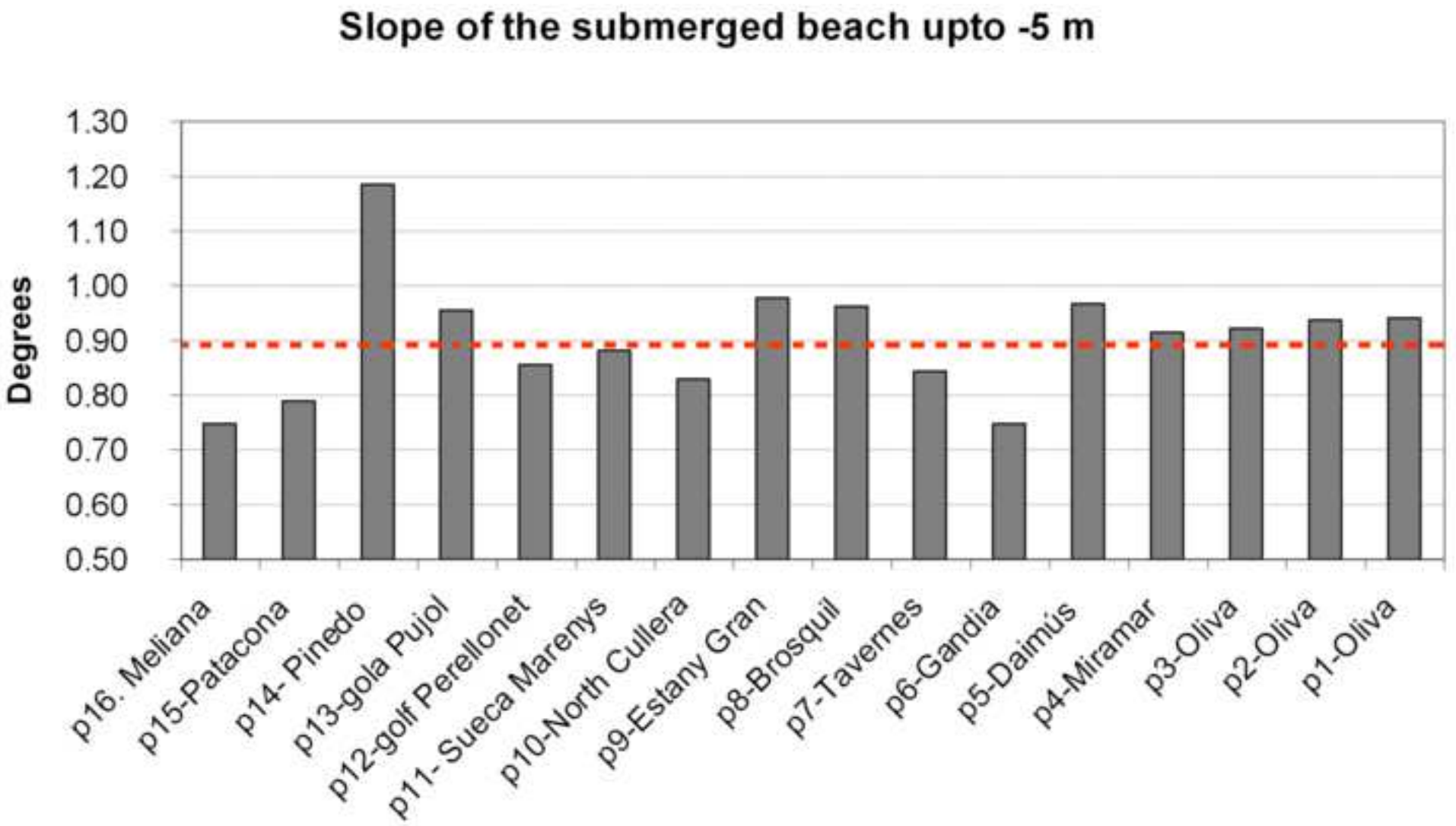

Figure 3 (colour)
Click here to download high resolution image

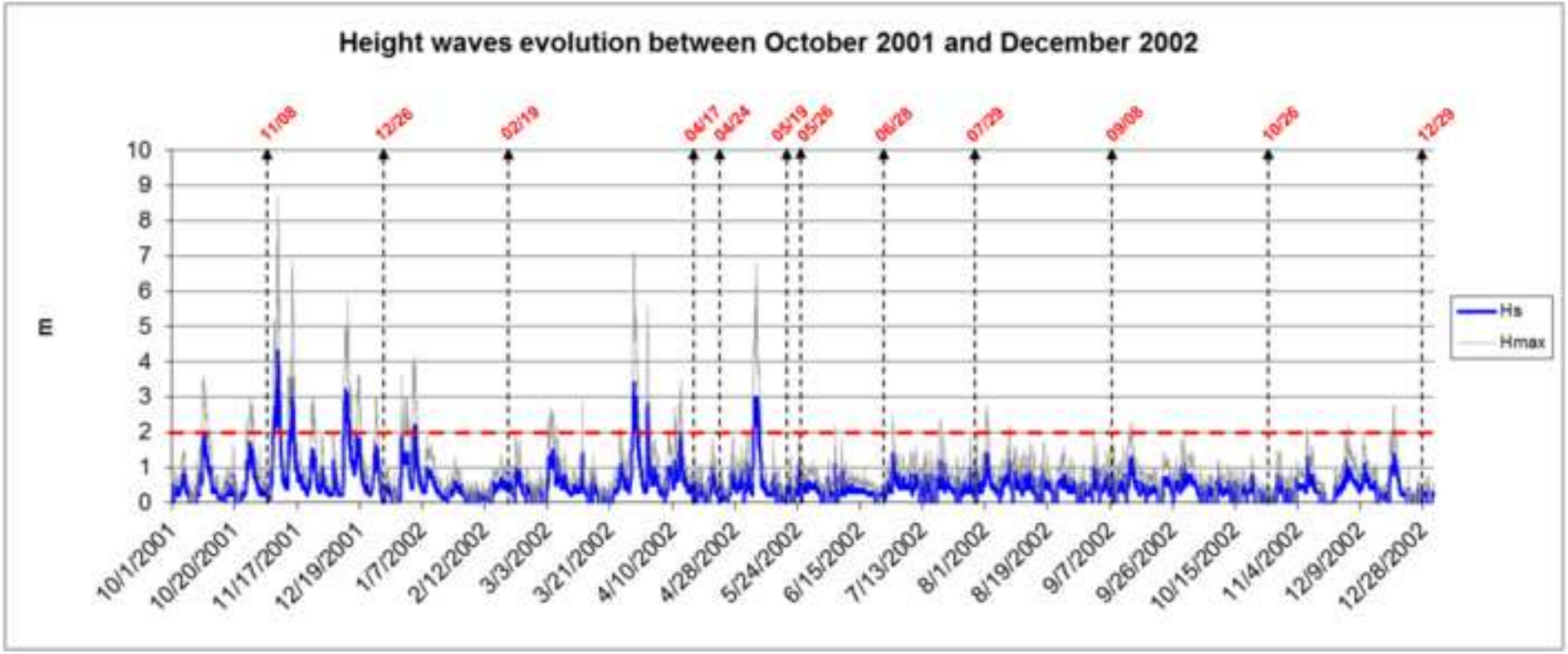

Figure 4 (colour)
Click here to download high resolution image

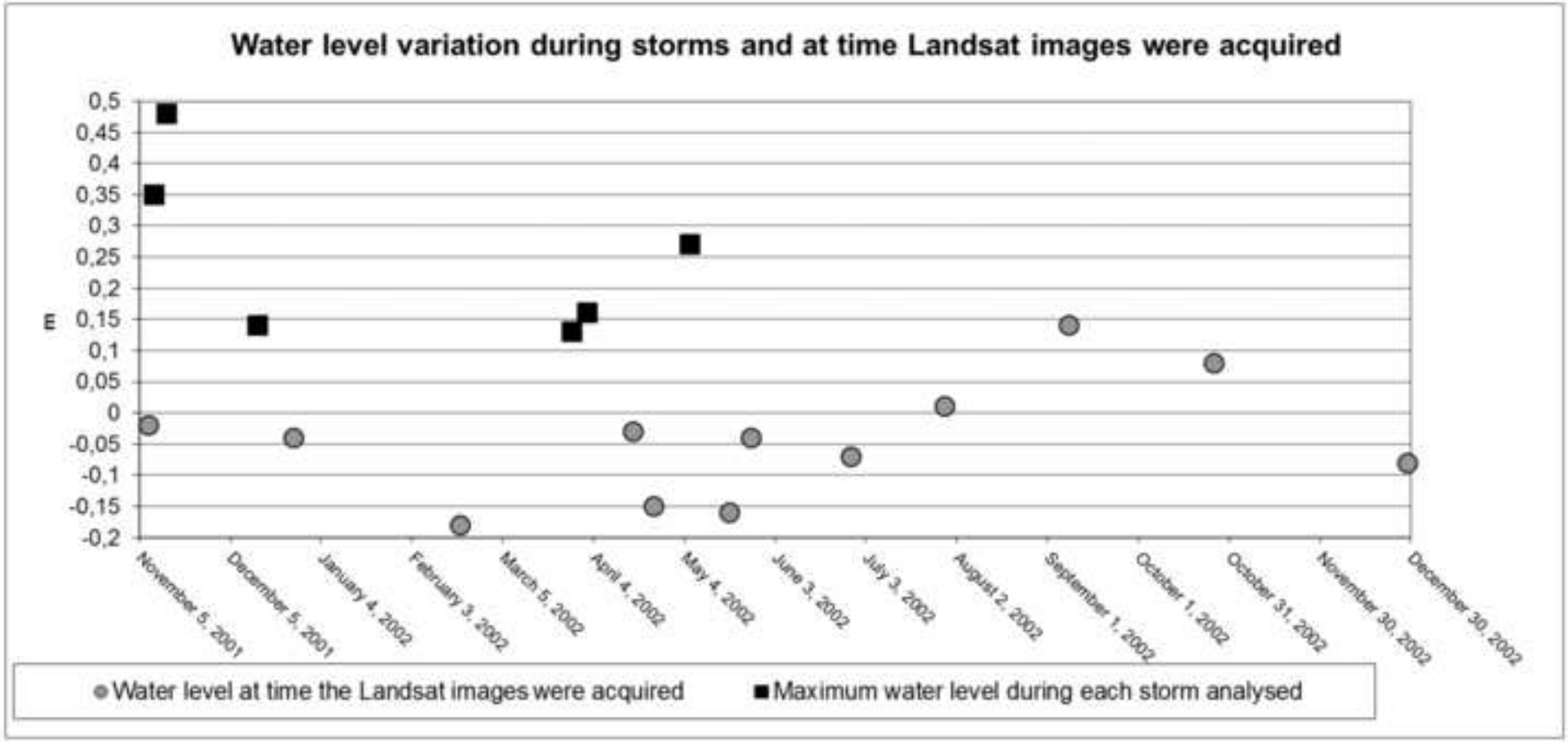

Figure 5 (colour)

Click here to download high resolution image

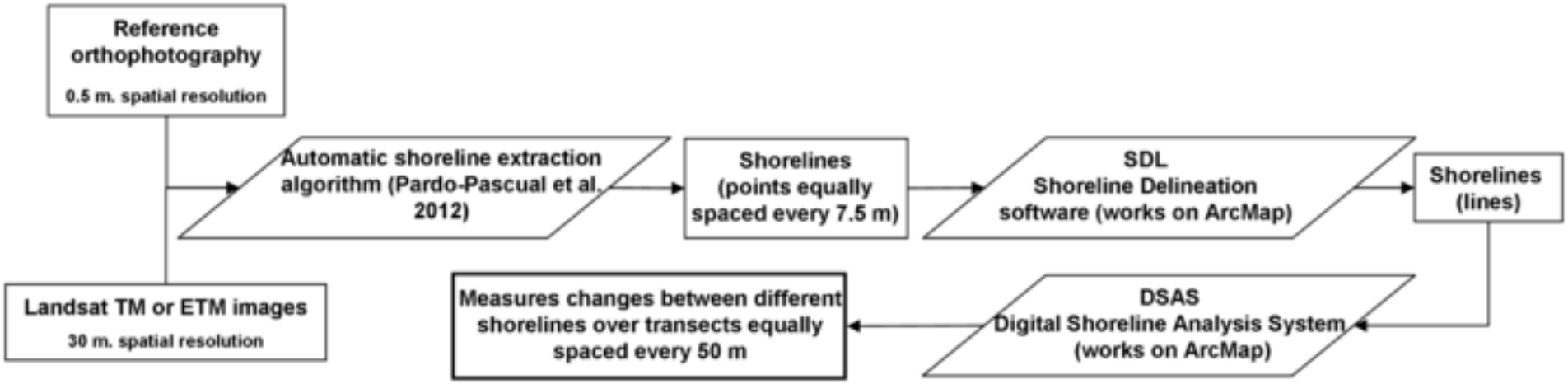

Figure 6 (colour)
Click here to download high resolution image

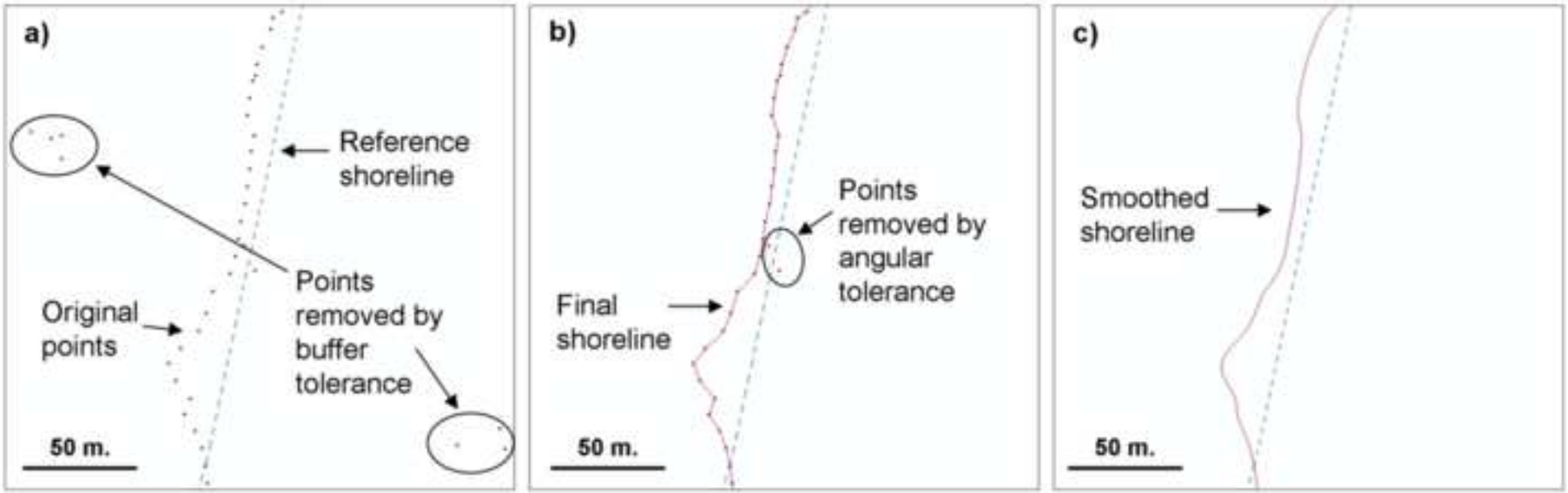

Figure 7 (colour)
Click here to download high resolution image

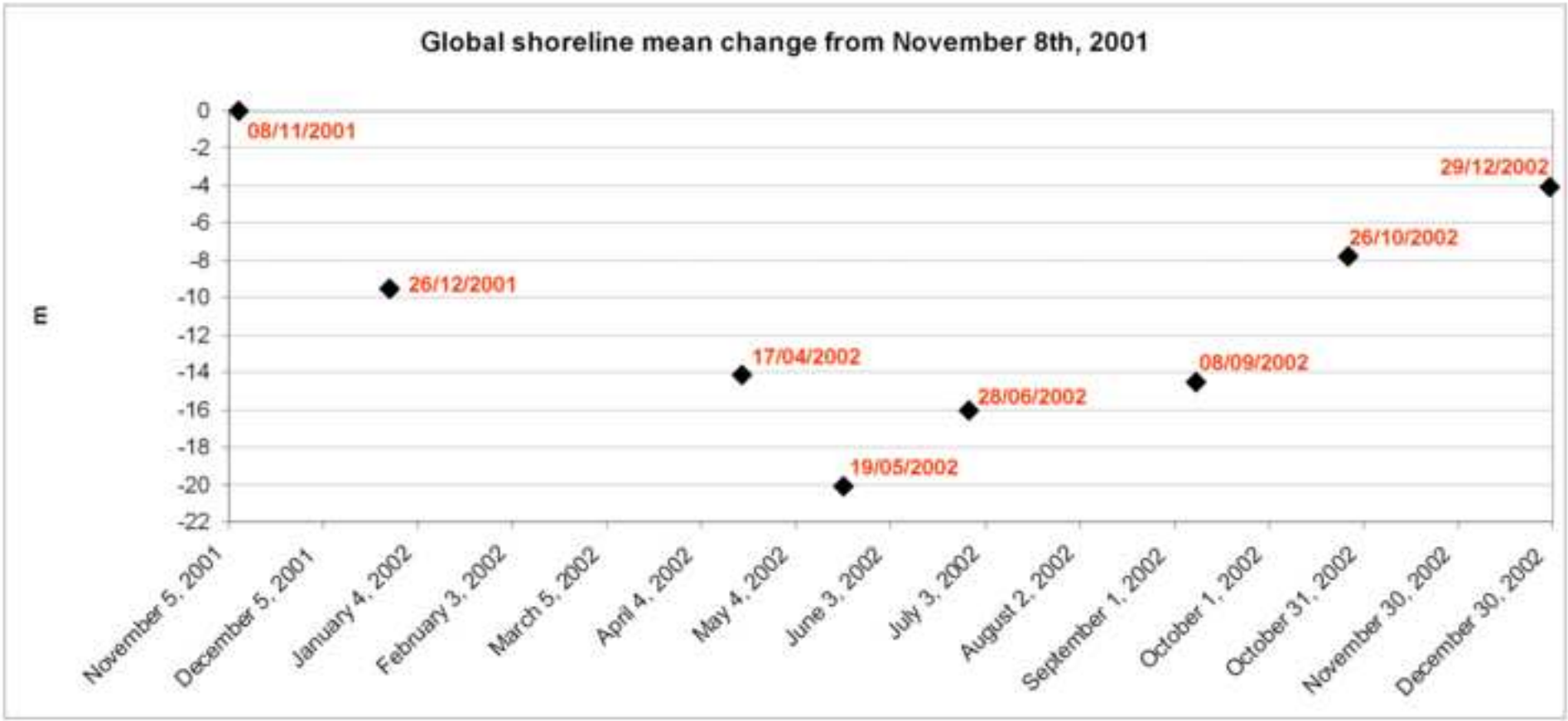

Figure 8 (colour)

Click here to download high resolution image

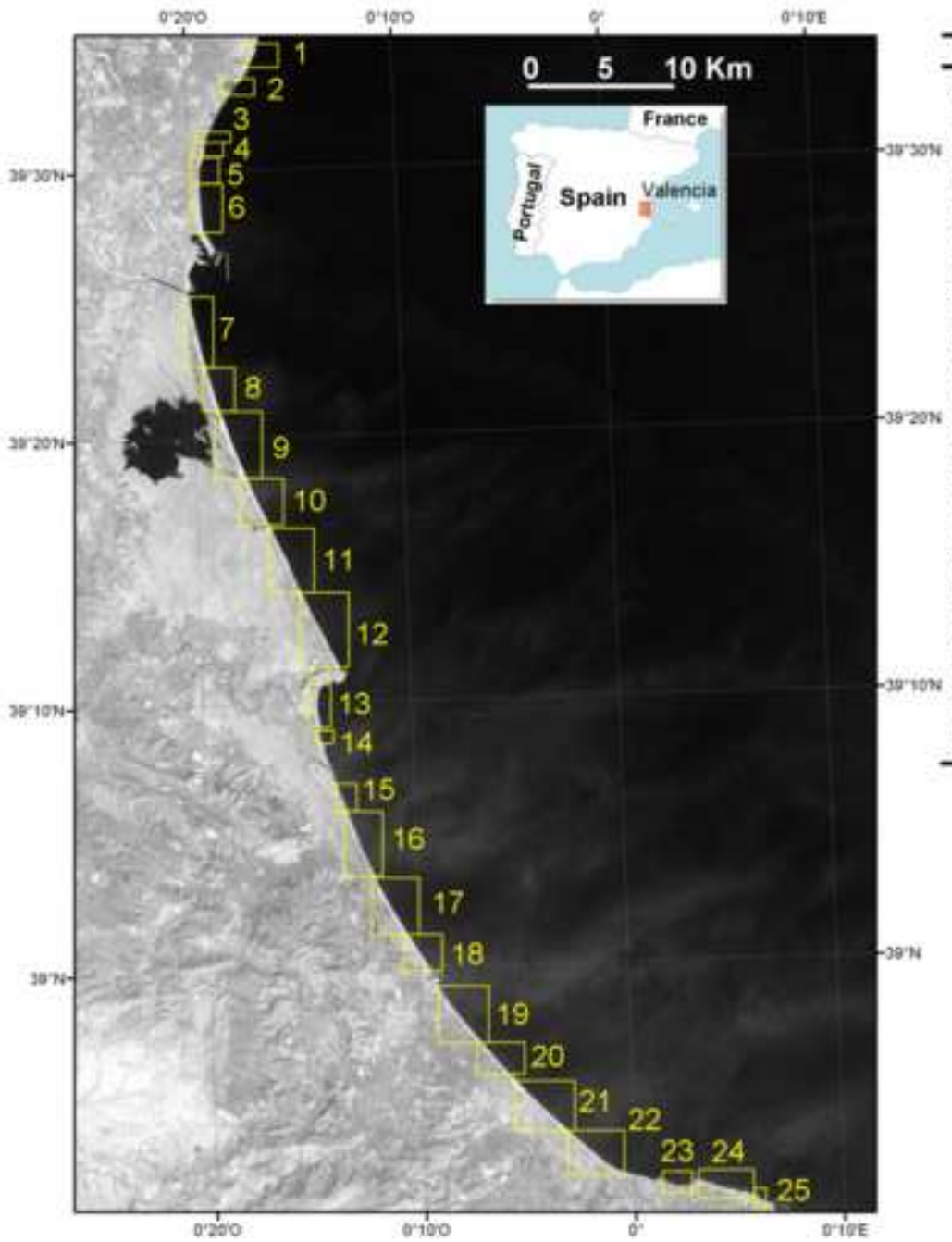

Zone	Local names	Length (m)
Zone 1	Border north study area to Port Pobla Farnals	1750
Zone 2	Port Pobla Farnals to seawall Massalfassar	1550
Zone 3	Meliana beach	700
Zone 4	Meliana to Port Saplaya	950
Zone 5	Port Saplaya to edge Patacona beach	1850
Zone 6	Patacona beach to Port of Valencia	3350
Zone 7	North Devesa del Saler	5000
Zone 8	Devesa del Saler (until Pujol inlet)	3050
Zone 9	Pujol inlet to Perellonet inlet	4900
Zone 10	Perellonet inlet to Perelló inlet	3400
Zone 11	Perelló inlet to south Mareny Barraquetes	4950
Zone 12	Mareny de Barraquetes to Cape Cullera	5750
Zone 13	Cape Cullera to river Xúquer mouth	3300
Zone 14	River Xúquer mouth to Platja del Marenyet (Cullera)	850
Zone 15	Brosquil to Goleta Tavernes	2000
Zone 16	Goleta de Tavernes to Séquia de la Ratlla Xeraco	4800
Zone 17	Xeraco to end Platja de l'Auir (Gandia)	4500
Zone 18	Platja de l'Auir to port of Gandia	2950
Zone 19	Port of Gandia to border Piles municipality	5000
Zone 20	Border Piles to la Goleta d'Oliva marina	2750
Zone 21	Goleta d'Oliva to Santa Anna beach (Oliva Nova)	5000
Zone 22	Santa Anna beach to les Deveses (Dénia)	4850
Zone 23	La Punta dels Molins	2250
Zone 24	Les Bassetes (Dénia)	3900
Zone 25	Les Bassetes to Dénia port	900

Figure 9 (colour)

Click here to download high resolution image

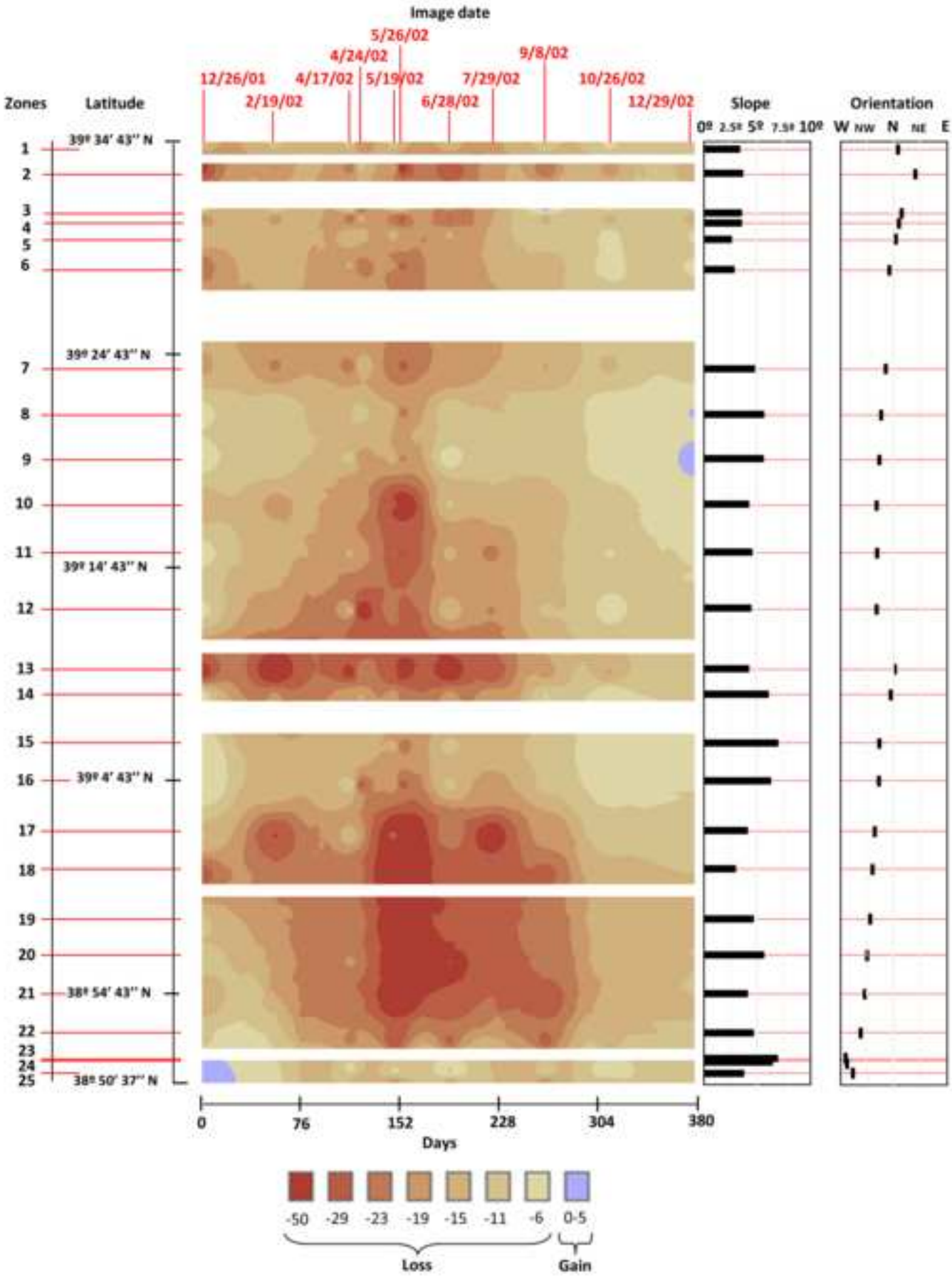

Figure 10 (colour)
Click here to download high resolution image

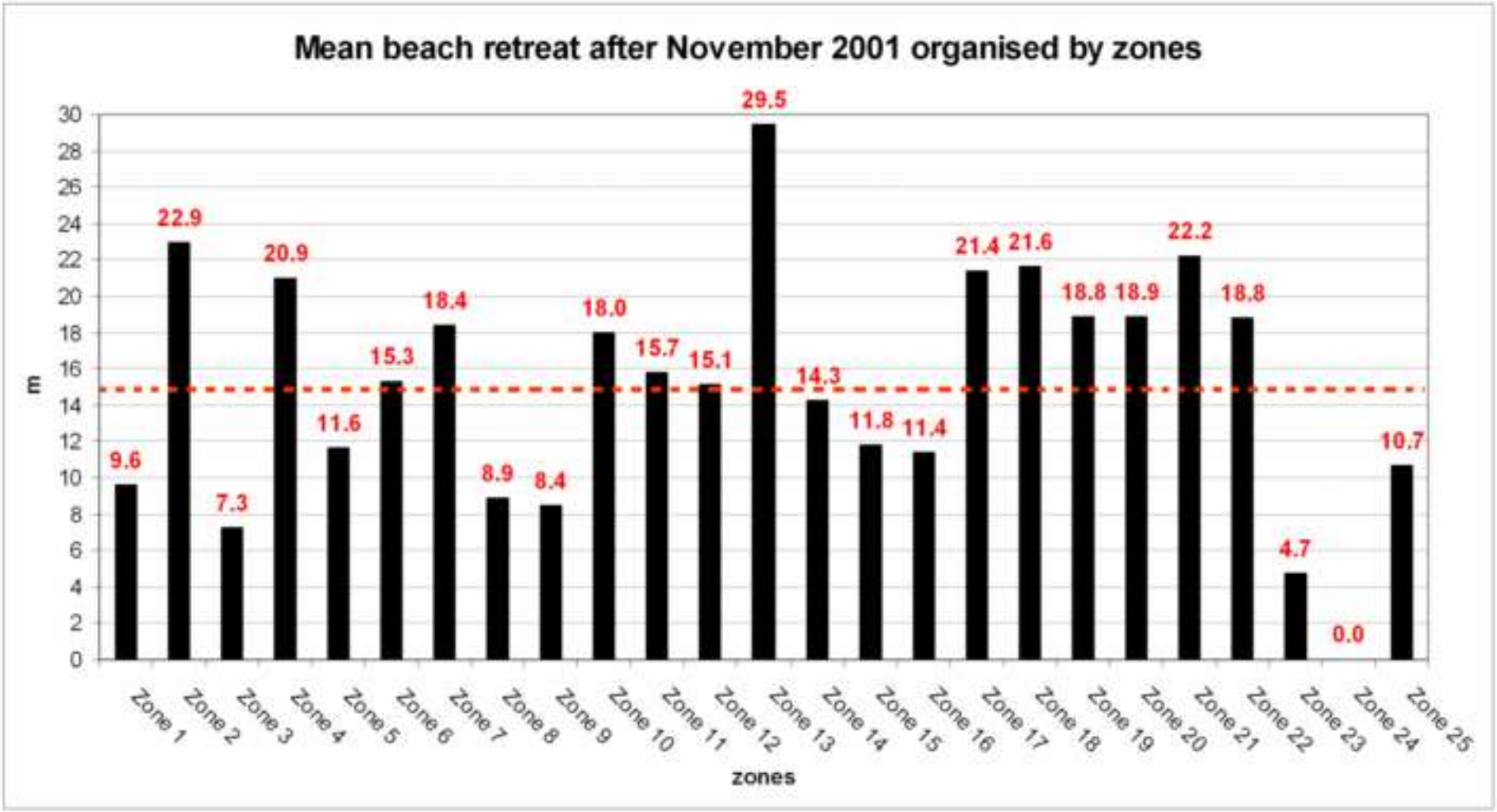

Figure 11 colour (modified)
Click here to download high resolution image

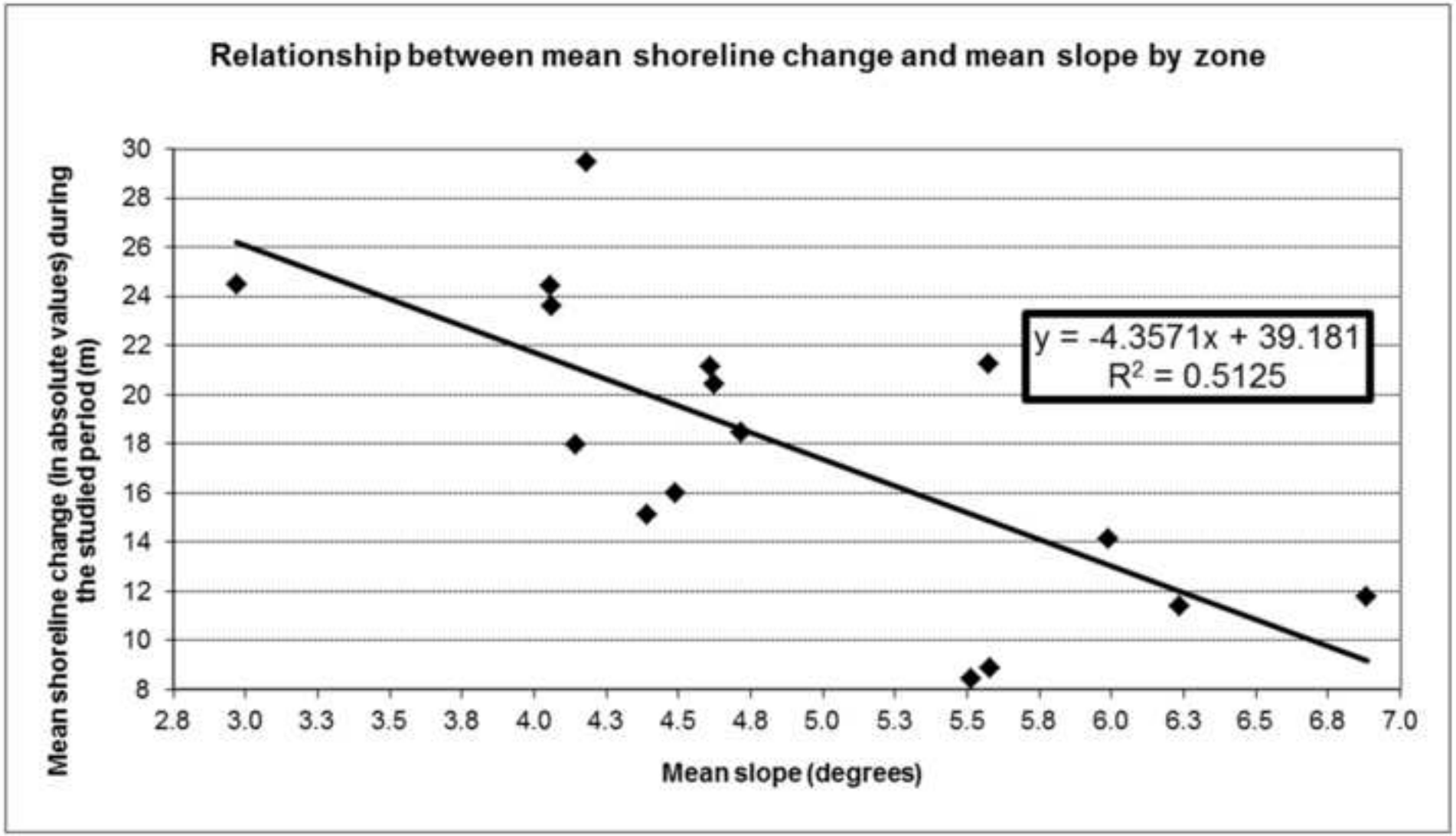

Figure 12 (colour)
Click here to download high resolution image

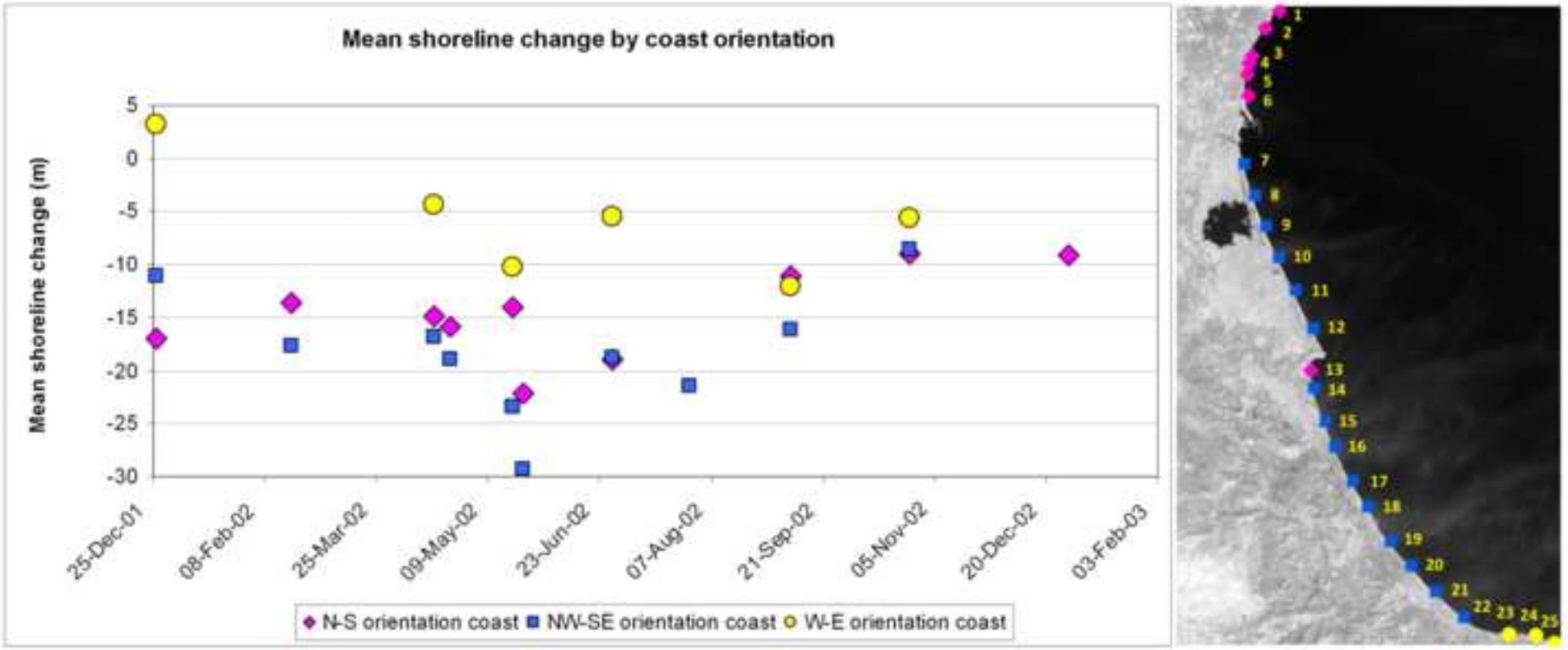

Figure 13 (colour)
Click here to download high resolution image

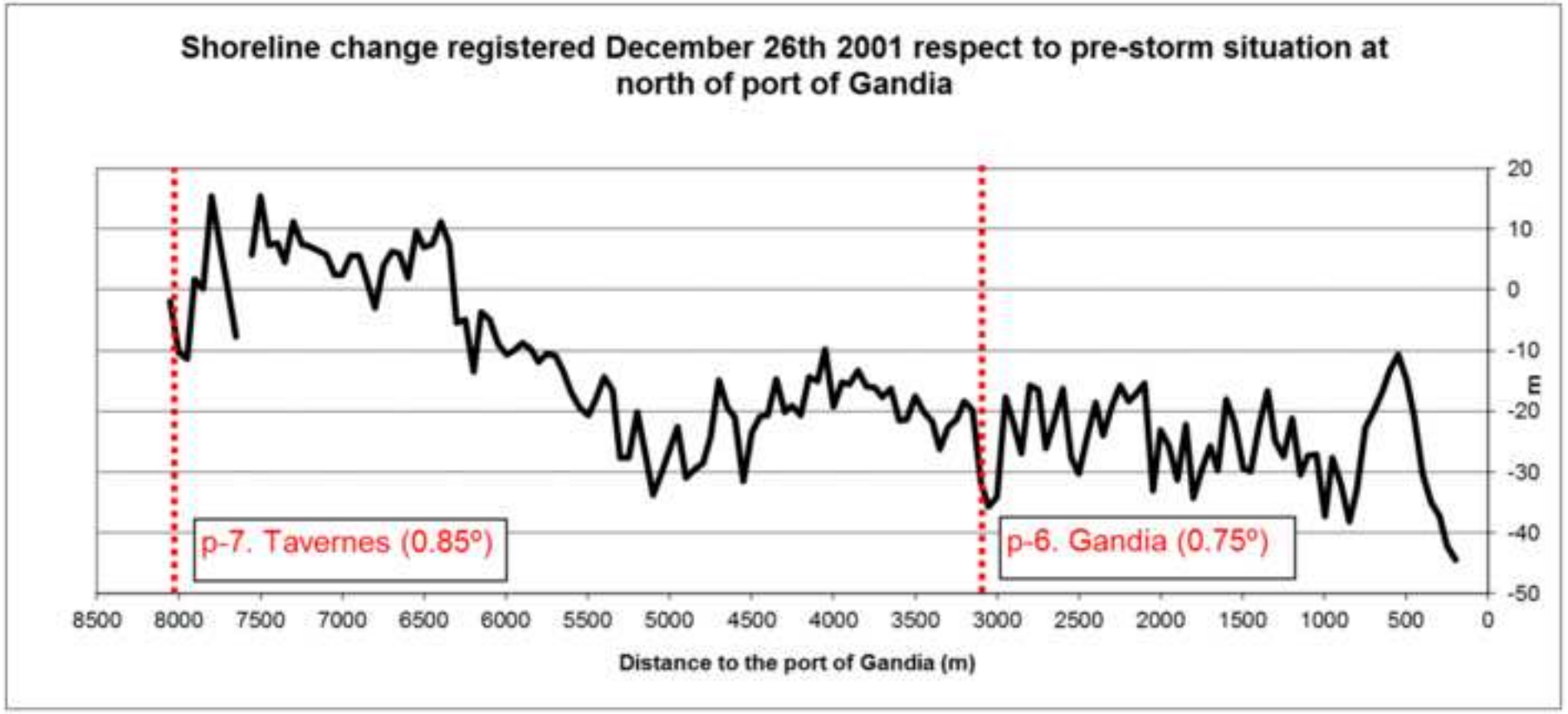

Figure 1 (B/W)

Click here to download high resolution image

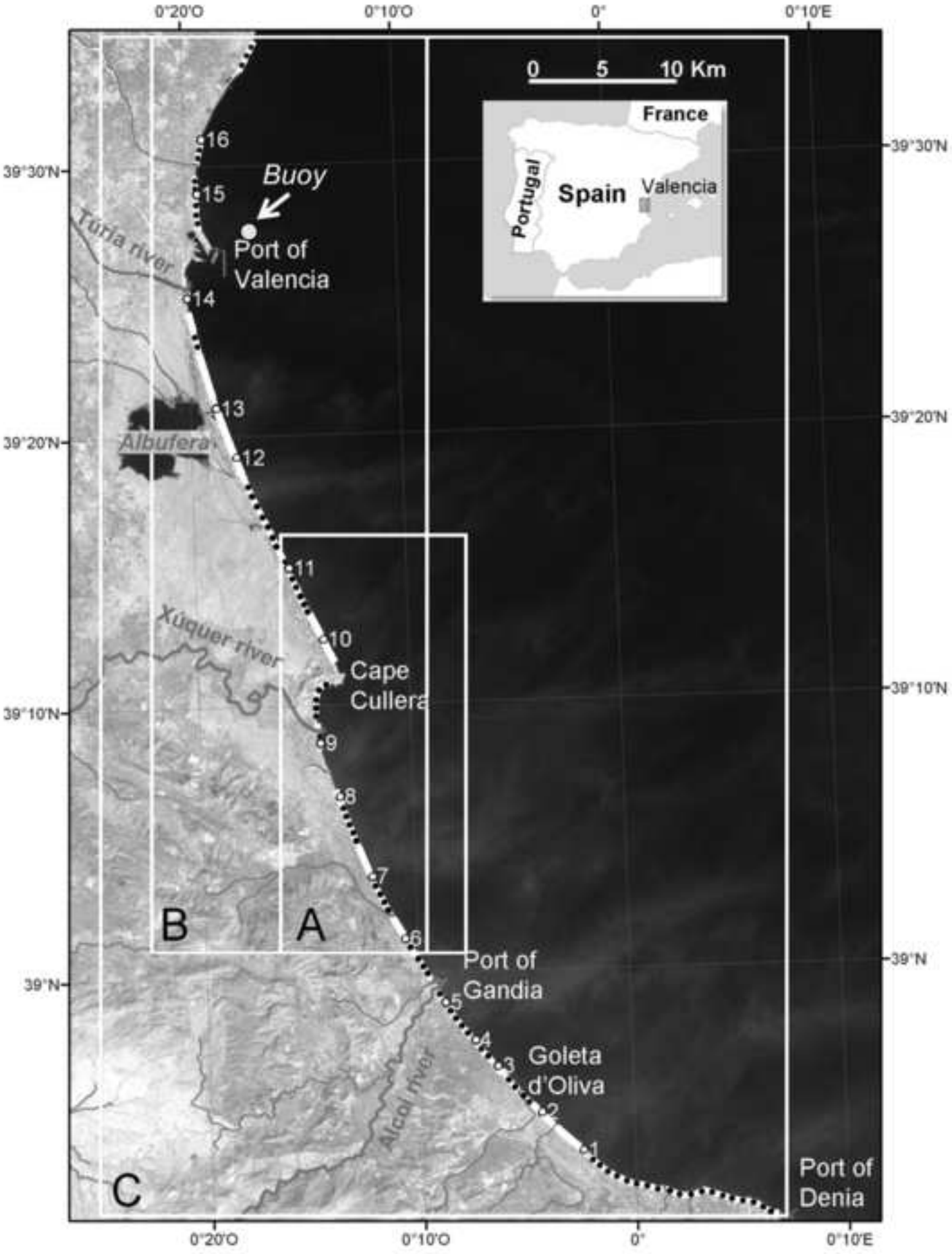

Figure 2 (B/W)
Click here to download high resolution image

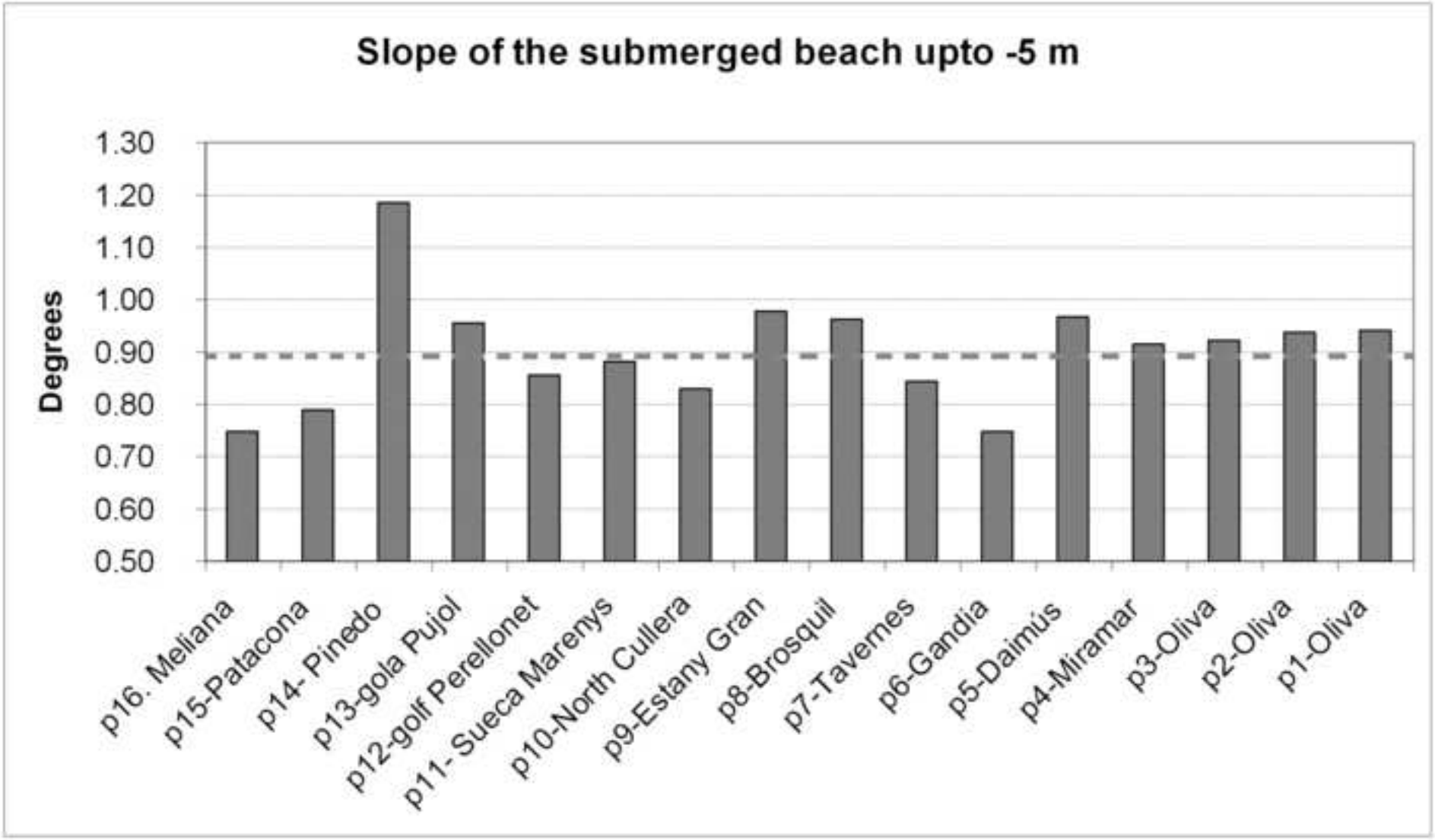

Figure 3 (B/W)

Click here to download high resolution image

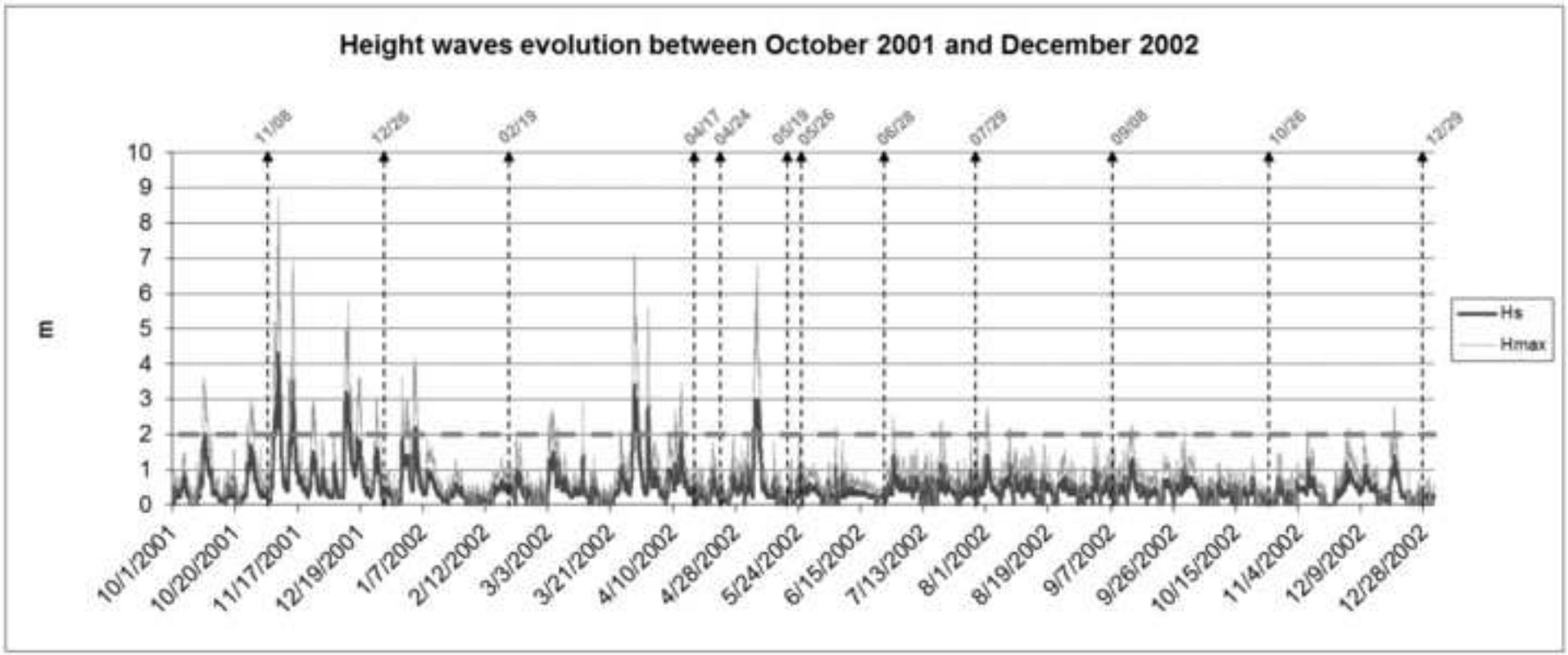

Figure 4 (B/W)

Click here to download high resolution image

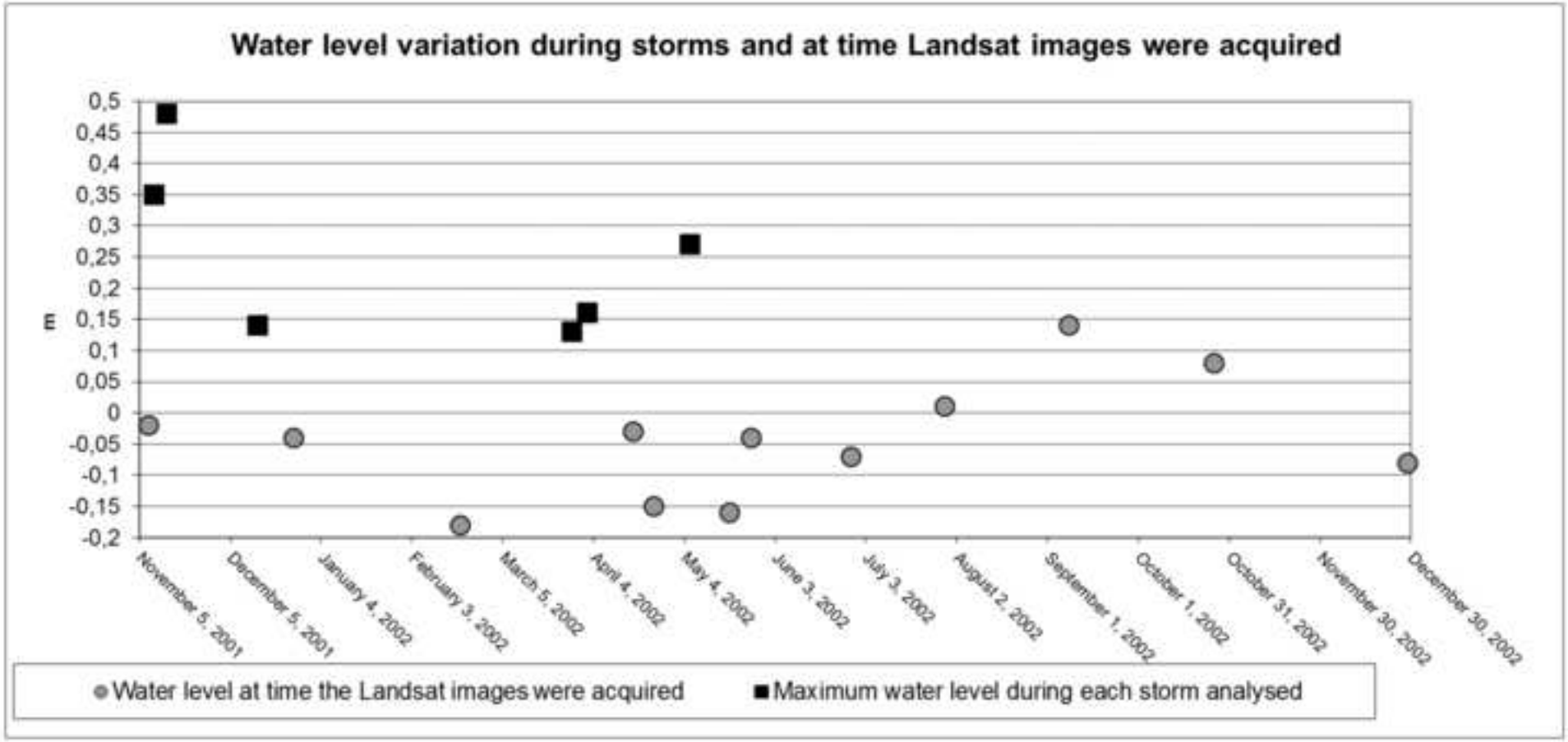

Figure 5 (B/W)

Click here to download high resolution image

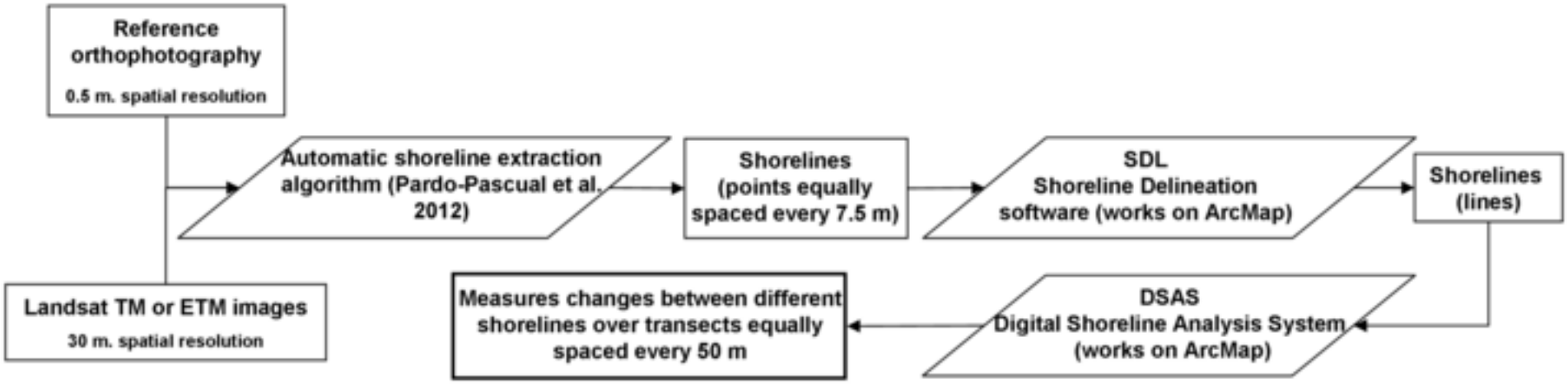

Figure 6 (B/W)
Click here to download high resolution image

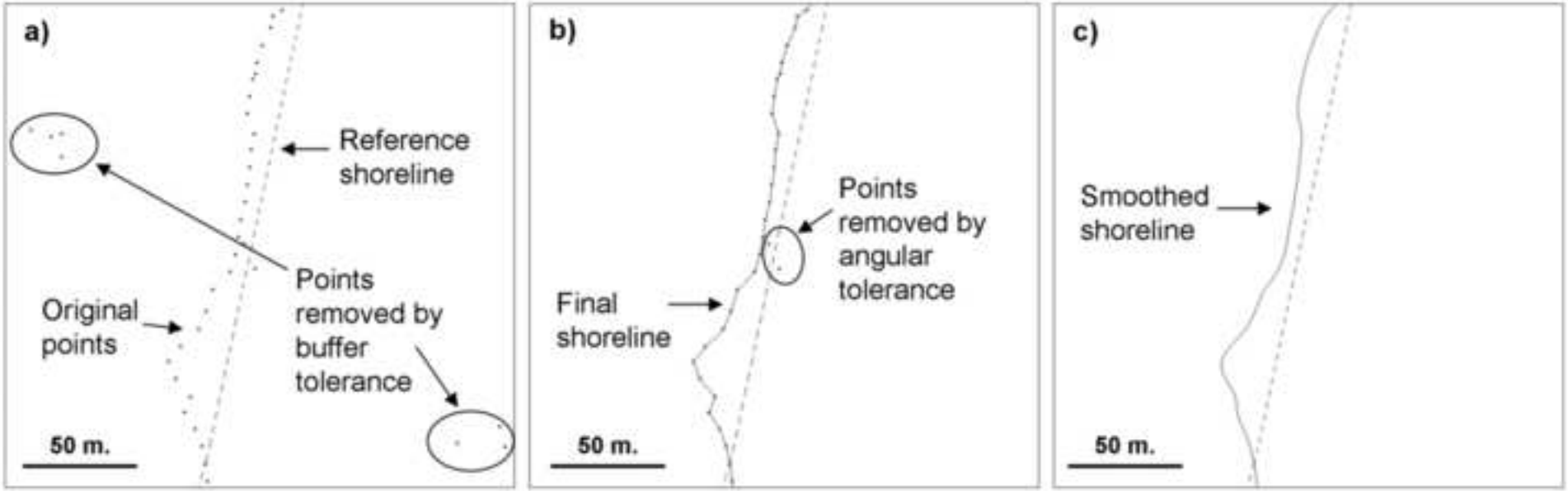

Figure 7 (B/W)
Click here to download high resolution image

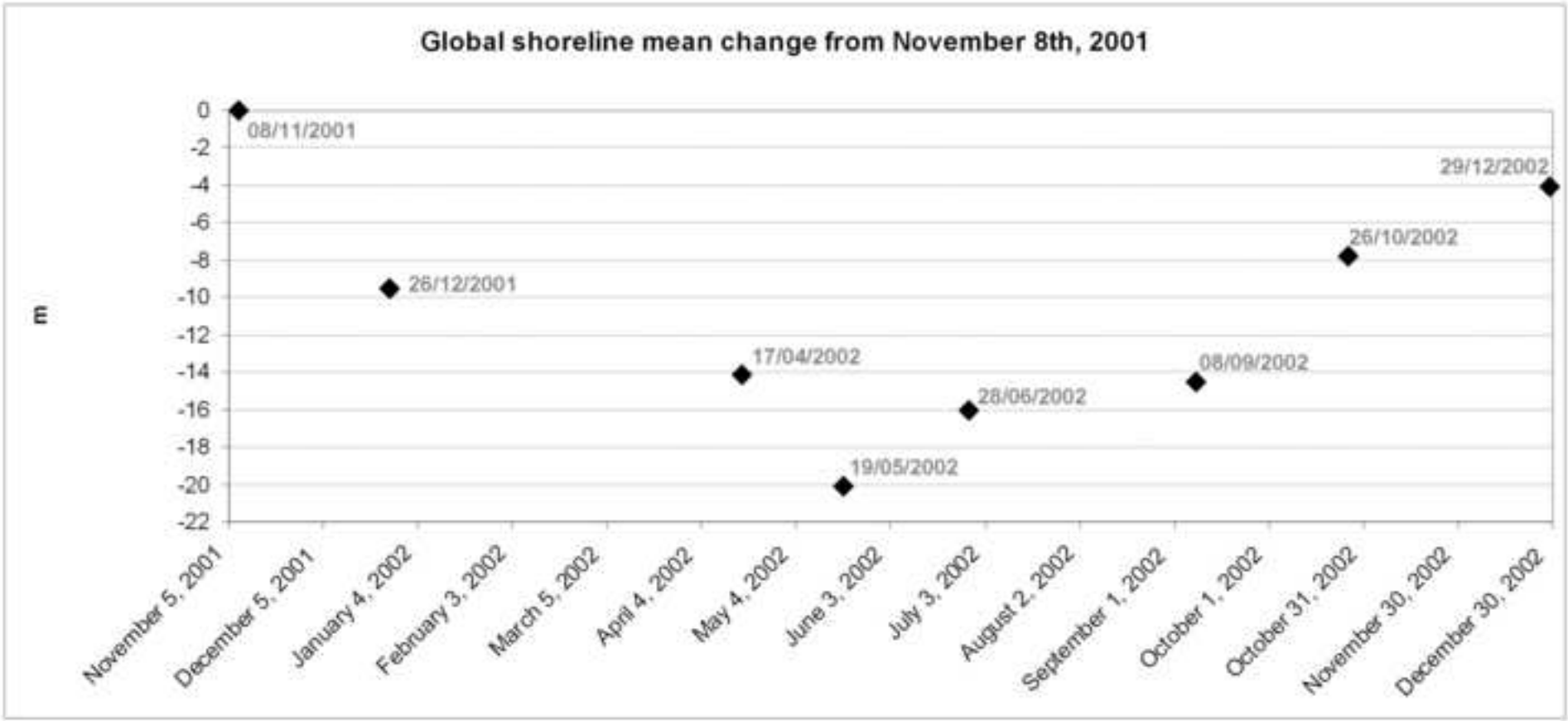

Figure 8 (B/W)

Click here to download high resolution image

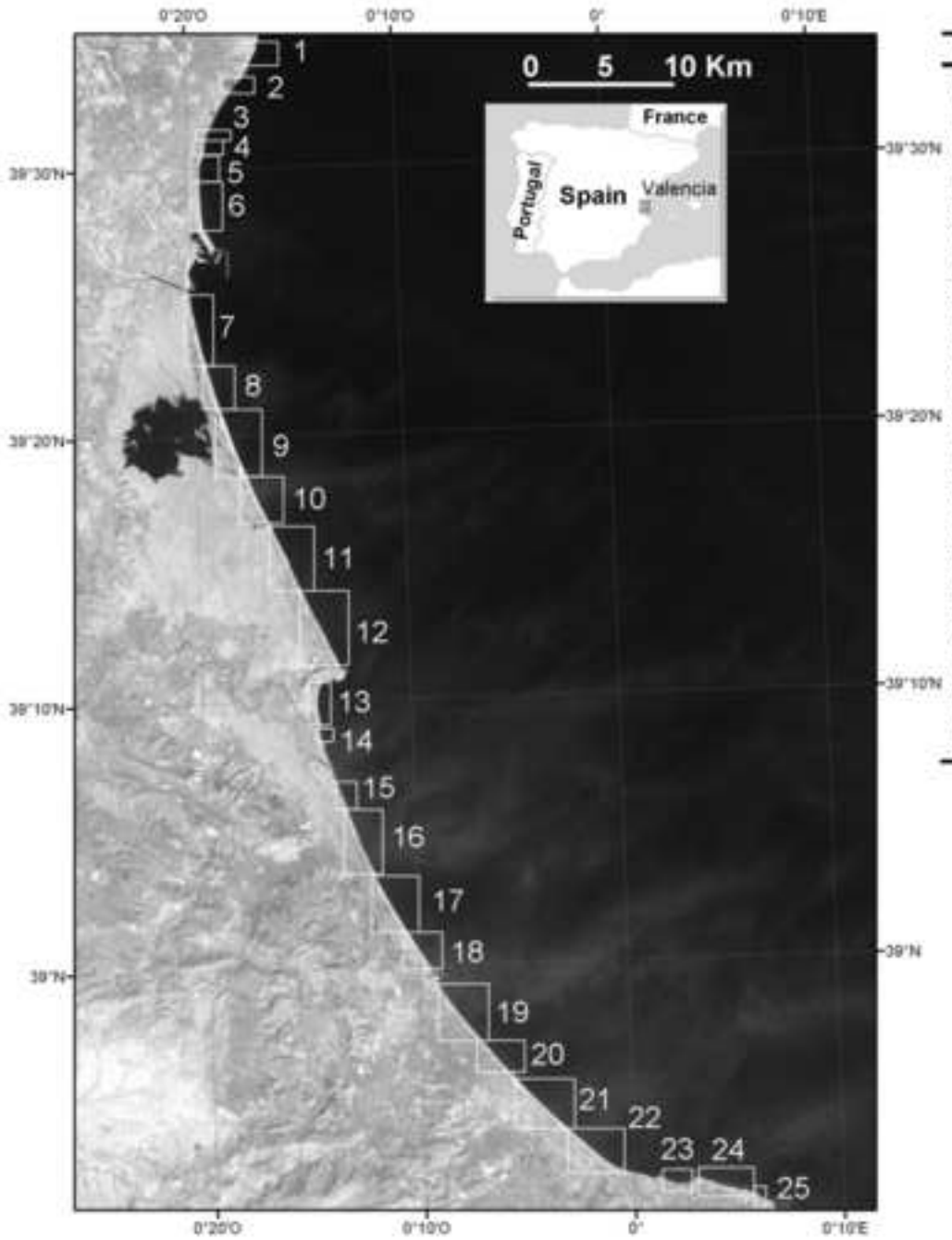

Zone	Local names	Length (m)
Zone 1	Border north study area to Port Pobla Farnals	1750
Zone 2	Port Pobla Farnals to seawall Massalfassar	1550
Zone 3	Meliana beach	700
Zone 4	Meliana to Port Saplaya	950
Zone 5	Port Saplaya to edge Patacona beach	1850
Zone 6	Patacona beach to Port of Valencia	3350
Zone 7	North Devesa del Saler	5000
Zone 8	Devesa del Saler (until Pujol inlet)	3050
Zone 9	Pujol inlet to Perellonet inlet	4900
Zone 10	Perellonet inlet to Perelló inlet	3400
Zone 11	Perelló inlet to south Mareny Barraquetes	4950
Zone 12	Mareny de Barraquetes to Cape Cullera	5750
Zone 13	Cape Cullera to river Xúquer mouth	3300
Zone 14	River Xúquer mouth to Platja del Marenyet (Cullera)	850
Zone 15	Brosquil to Goleta Tavernes	2000
Zone 16	Goleta de Tavernes to Séquia de la Ratlla Xeraco	4800
Zone 17	Xeraco to end Platja de l'Auir (Gandia)	4500
Zone 18	Platja de l'Auir to port of Gandia	2950
Zone 19	Port of Gandia to border Piles municipality	5000
Zone 20	Border Piles to la Goleta d'Oliva marina	2750
Zone 21	Goleta d'Oliva to Santa Anna beach (Oliva Nova)	5000
Zone 22	Santa Anna beach to les Deveses (Dénia)	4850
Zone 23	La Punta dels Molins	2250
Zone 24	Les Bassetes (Dénia)	3900
Zone 25	Les Bassetes to Dénia port	900

Figure 9 (B/W)

Click here to download high resolution image

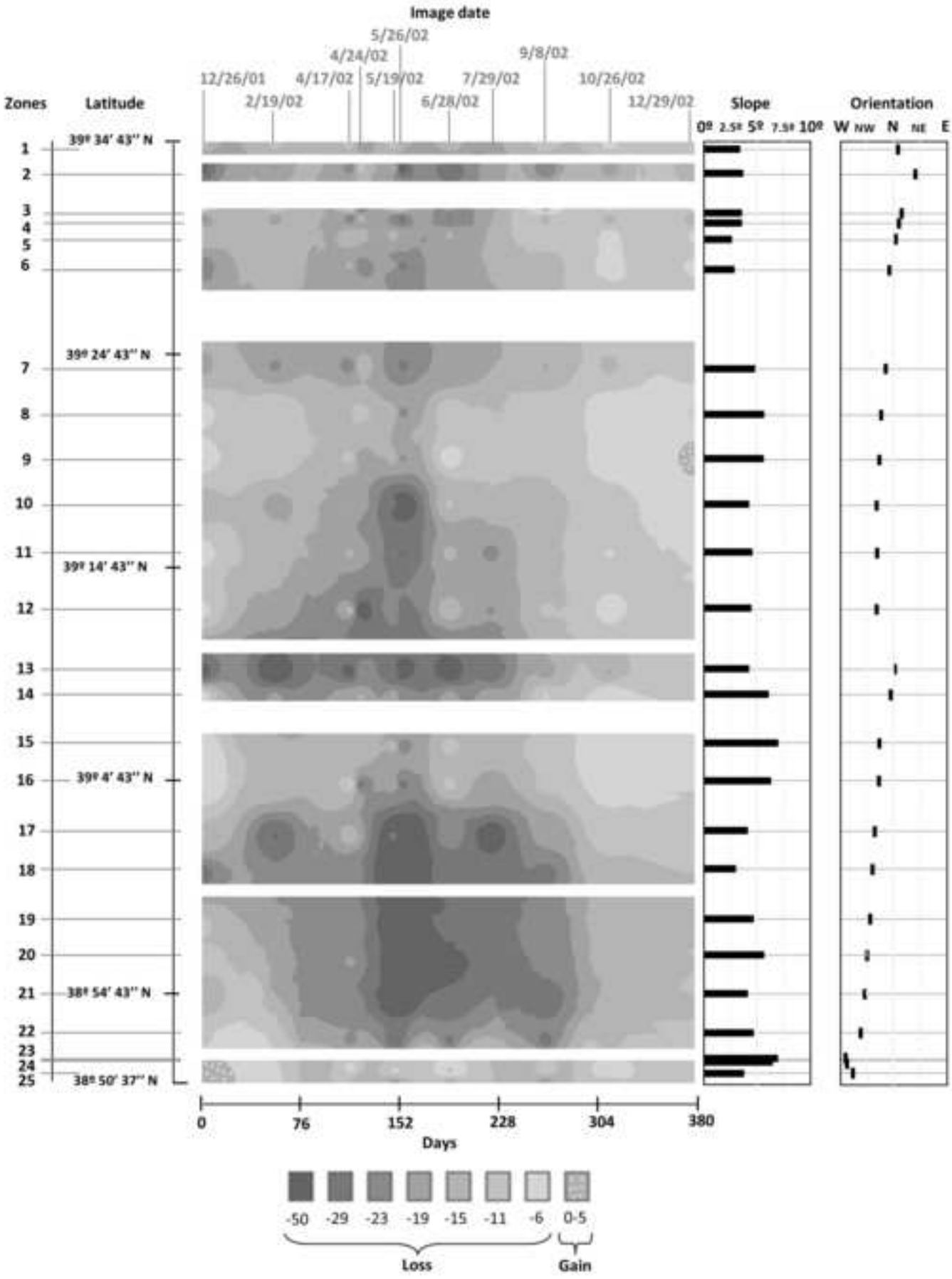

Figure 10 (B/W)
Click here to download high resolution image

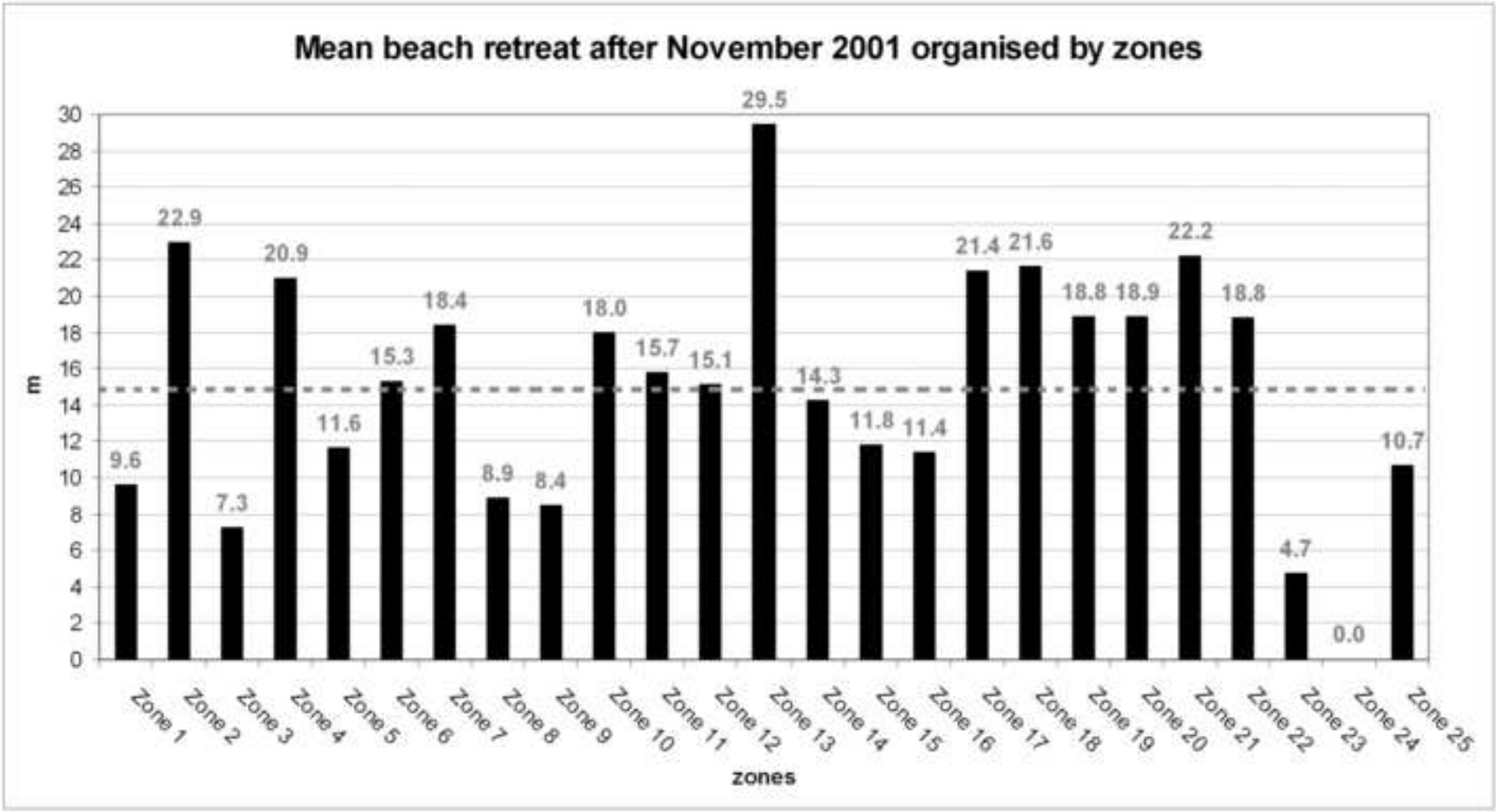

Figure 11 BW (modified)
Click here to download high resolution image

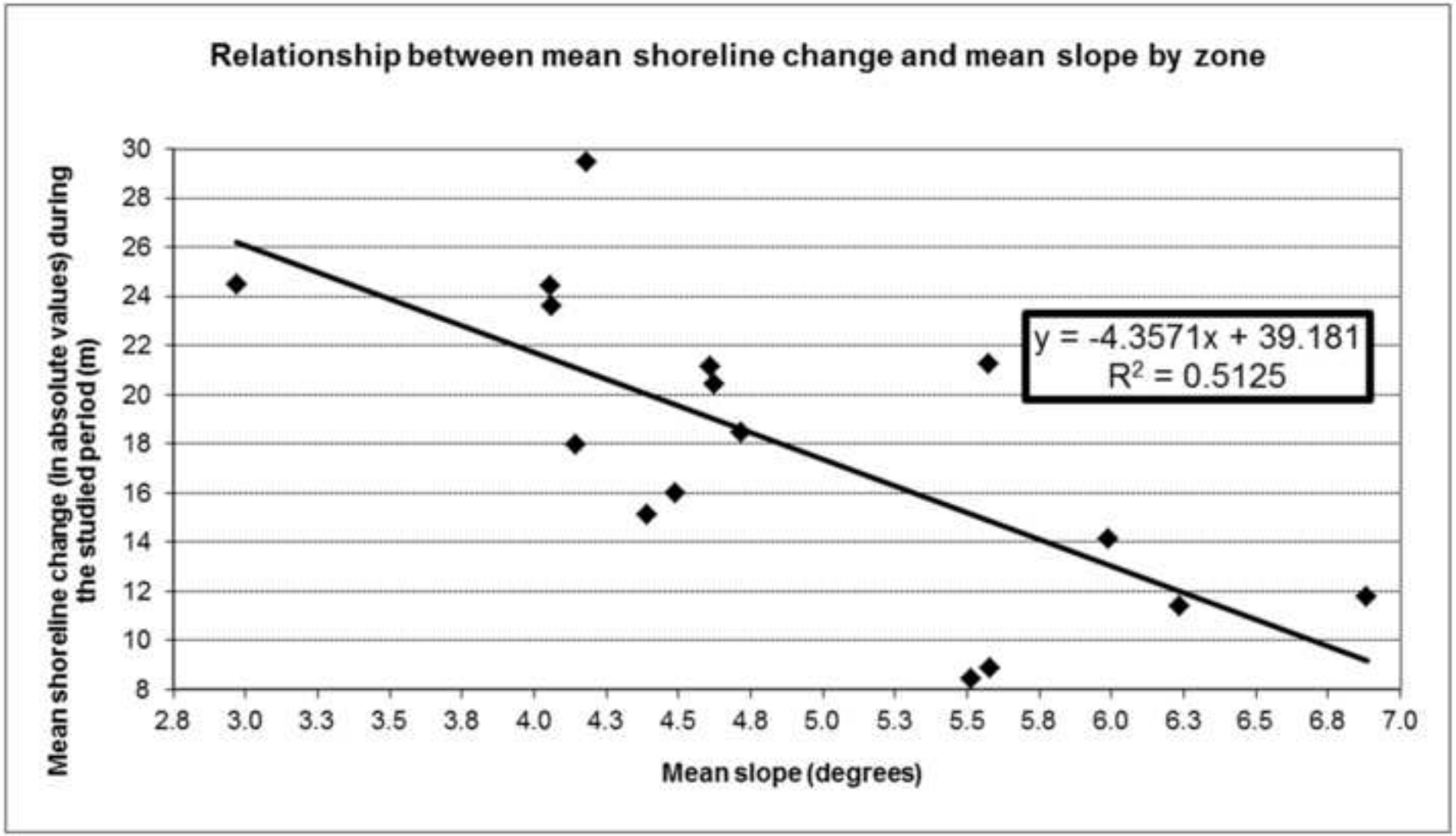

Figure 12 (B/W)

Click here to download high resolution image

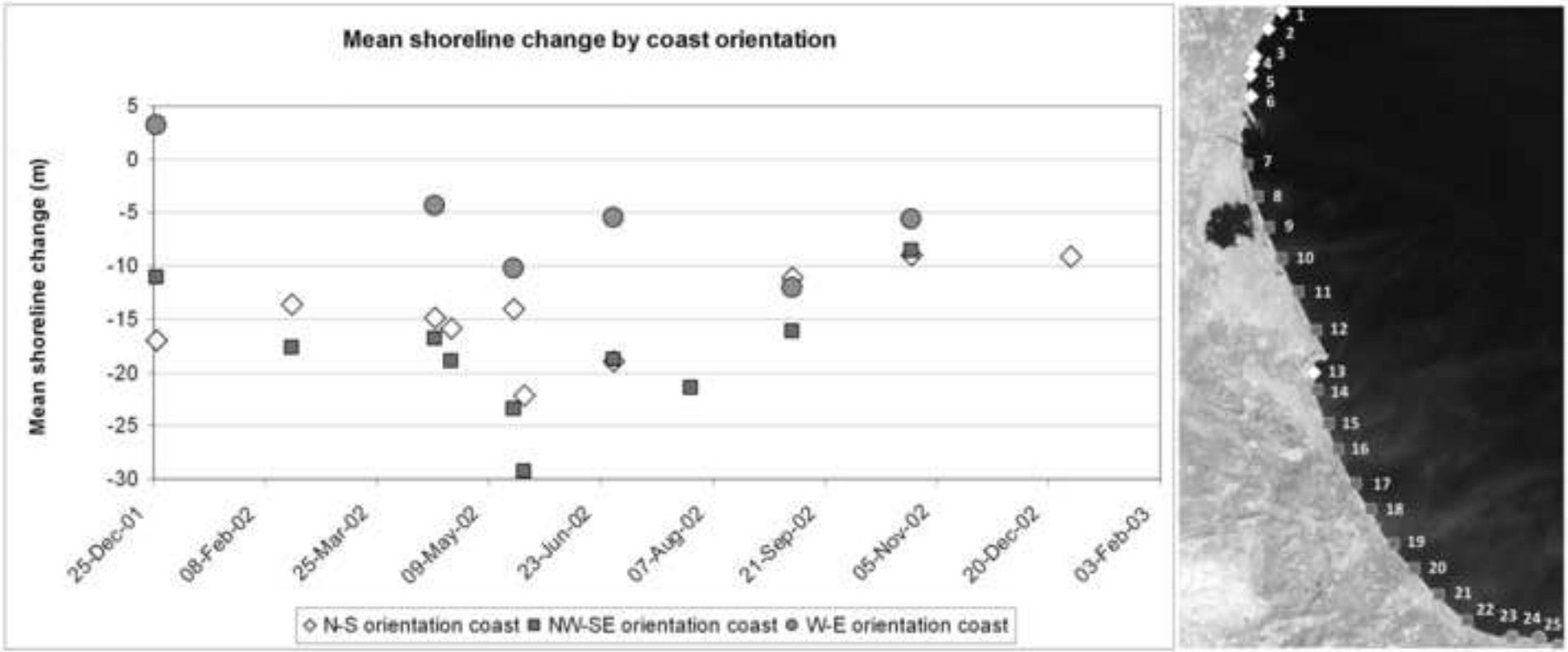

Figure 13 (B/W)
Click here to download high resolution image

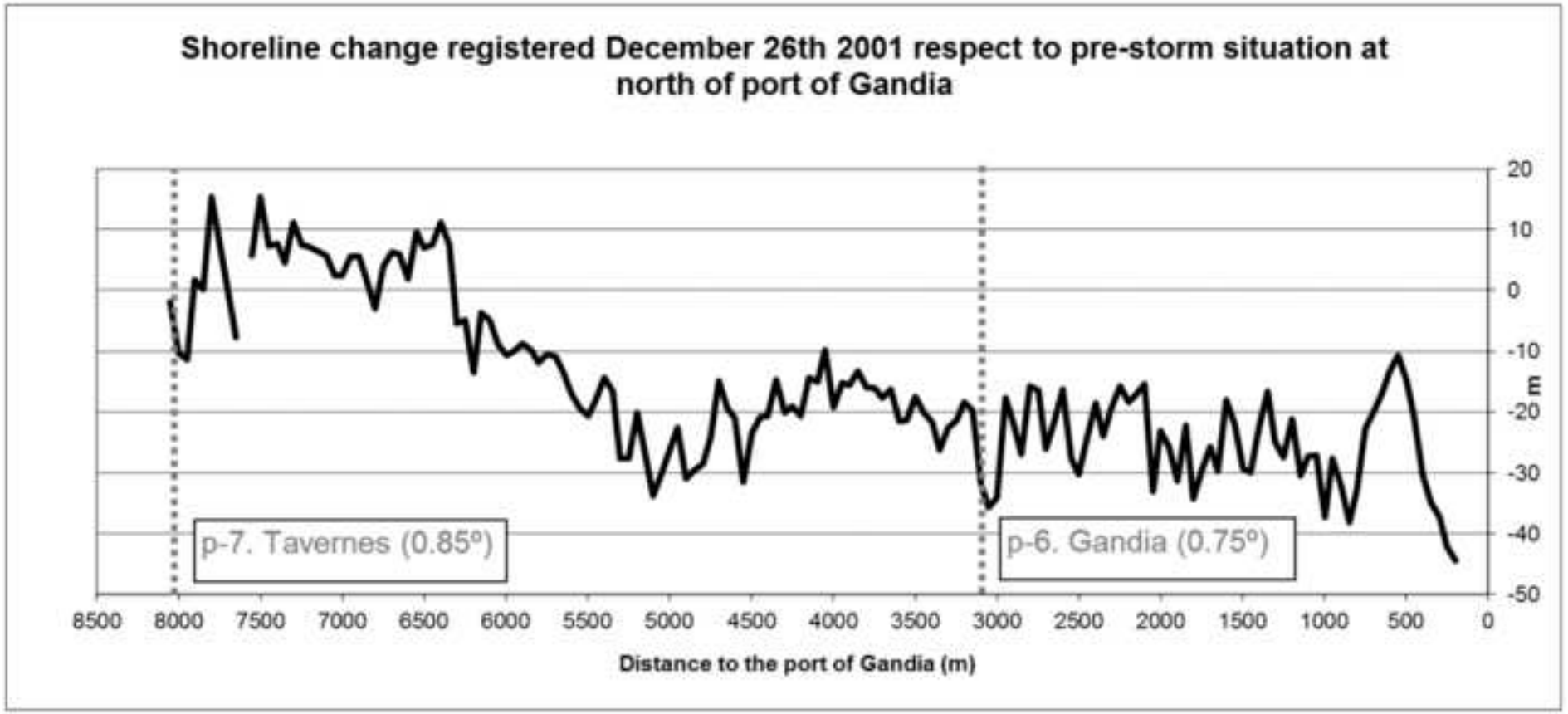

KML File (for GoogleMaps).Coastal types in the study area

Click here to download KML File (for GoogleMaps): type.kmz

KML File (for GoogleMaps). Areas

Click here to download KML File (for GoogleMaps): areas.kmz

KML File (for GoogleMaps). Landsat shorelines

Click here to download KML File (for GoogleMaps): shorelines.kmz

KML File (for GoogleMaps). Study zones

Click here to download KML File (for GoogleMaps): study_zones.kmz